Pleiotropic effects of the vacuolar ABC transporter *MLT1* of *Candida albicans* on cell function and virulence

Nitesh Kumar Khandelwal*, Philipp Kaemmer†, Toni M. Förster†, Ashutosh Singh‡§, Alix T. Coste∥, David R. Andes¶**, Bernhard Hube†, Dominique Sanglard∥, Neeraj Chauhan††, Rupinder Kaur‡‡, Christophe d'Enfert§§, Alok Kumar Mondal* and Rajendra Prasad∥∥[1]

*School of Life Sciences, Jawaharlal Nehru University, New Delhi 110067, India
†Department of Microbial Pathogenicity Mechanisms, Leibniz Institute for Natural Product Research and Infection Biology, Hans Knoell Institute Jena (HKI), D-07745 Jena, Germany
‡Department of Molecular Genetics and Microbiology, Stony Brook University, 145 Life Sciences Building, Stony Brook, NY 11794, U.S.A.
§Department of Biochemistry, Lucknow University, Lucknow 226024, Uttar Pradesh, India
∥Institute of Microbiology, University of Lausanne and University Hospital Center, Rue du Bugnon 48, Lausanne, CH-1011, Switzerland
¶Division of Infectious Diseases, Department of Medicine, University of Wisconsin, Madison, WI 53792, U.S.A.
**Department of Medical Microbiology and Immunology, University of Wisconsin, Madison, WI 53706, U.S.A.
††Department of Microbiology and Molecular Genetics, Public Health Research Institute, New Jersey Medical School, Rutgers, The State University of New Jersey, 225 Warren Street, Newark, NJ 07103, U.S.A.
‡‡Laboratory of Fungal Pathogenesis, Centre for DNA Fingerprinting and Diagnostics, Hyderabad 500001, Andhra Pradesh, India
§§Département Génomes et Génétique, Institut Pasteur, Unité Biologie et Pathogénicité Fongiques, Paris, France, INRA, USC2019, Paris, France
∥∥Amity Institute of Integrative Sciences and Health, Amity University Haryana, Amity Education Valley, Gurgaon 122413, India

Among the several mechanisms that contribute to MDR (multidrug resistance), the overexpression of drug-efflux pumps belonging to the ABC (ATP-binding cassette) superfamily is the most frequent cause of resistance to antifungal agents. The multidrug transporter proteins Cdr1p and Cdr2p of the ABCG subfamily are major players in the development of MDR in *Candida albicans*. Because several genes coding for ABC proteins exist in the genome of *C. albicans*, but only Cdr1p and Cdr2p have established roles in MDR, it is implicit that the other members of the ABC family also have alternative physiological roles. The present study focuses on an ABC transporter of *C. albicans*, Mlt1p, which is localized in the vacuolar membrane and specifically transports PC (phosphatidylcholine) into the vacuolar lumen. Transcriptional profiling of the *mlt1*Δ/Δ mutant revealed a down-regulation of the genes involved in endocytosis, oxidoreductase activity, virulence and hyphal development. High-throughput MS-based lipidome analysis revealed that the Mlt1p levels affect lipid homoeostasis and thus lead to a plethora of physiological perturbations. These include a delay in endocytosis, inefficient sequestering of reactive oxygen species (ROS), defects in hyphal development and attenuated virulence. The present study is an emerging example where new and unconventional roles of an ABC transporter are being identified.

Key words: ABC transporter, *Candida albicans*, *MLT1*, phosphotidylcholine, virulence.

INTRODUCTION

Only a few *Candida* species exist in humans commensally, and they may become pathogenic when the microbiota is unbalanced, epithelial barriers are disrupted or the immune system is weakened. Various categories of drugs, such as azoles, polyenes, allylamines, echinocandins and pyrimidine analogues, are being used to combat *Candida albicans* infections. The prolonged use of antifungal agents increases the probability that *Candida* species develop tolerance not only to the drugs to which they are exposed, but also to several other drugs. This phenomenon of MDR (multidrug resistance) is supported by the different strategies adopted by *Candida*, which include target alteration and the overexpression of its gene products. Among the various mechanisms of MDR, enhanced drug extrusion by resistant *Candida* cells represents a prominent strategy. Rapid drug extrusion by resistant *C. albicans* cells is the result of overexpression of the drug-efflux pump-encoding genes *CDR1* and *CDR2*, which belong to the ABC (ATP-binding cassette) and *MDR1* gene families within the MFS (major facilitator superfamily) of transporters [1–4].

The *C. albicans* genome is composed of 26 genes that encode putative ABC superfamily proteins belonging to the ABCB, ABCC, ABCD, ABCF, ABCE and ABCG major subfamilies. Only two members of this superfamily, Cdr1p and Cdr2p, which belong to the ABCG subfamily, are involved in clinical MDR. However, the presence of large numbers of proteins in the ABC and MFS classes suggests that they may have distinct physiological roles. These transporter proteins, particularly those belonging to the ABC superfamily, perform diverse functions. The functional diversity of these proteins is reflected by additional roles in absorption, excretion, signal

transduction and pathogenesis. For instance, ABC transporters such as ScPdr5 of *Saccharomyces cerevisiae* or Cdr1p and Cdr2p of *C. albicans*, are phospholipid translocators that maintain membrane asymmetry [5]. The *S. cerevisiae* transporter ScMdl1 is a peptide transporter, whereas ScSte6 exports a-factor pheromone [6,7]. The cryptococcal transporters CnItra1A and CnItra3C not only transport inositol but also affect its virulence [8]. The *Cryptococcus neoformans* ABC transporter gene *CnAFR1* provides resistance to fluconazole and is involved in the delayed phagosomal maturation of phagosomes containing *C. neoformans* cells [9,10]. The GDP-mannose transporters CnGmt1 and CnGmt2 of *C. neoformans* are involved in capsule synthesis [11]. The loss of abcB from *Aspergillus fumigatus* invariably elicits increased azole susceptibility and decreased virulence [12]. In *Dictyostelium discoideum*, the ABC transporter AmtA acts as an ammonia transporter and regulates ammonia homoeostasis [13]. The ammonium transporter Ump2 of the plant pathogen *Ustilago maydis* also interacts with the signalling protein Rho1, which controls polarized growth [14]. The vacuole transporter CgCtr2 of the plant pathogen *Colletotrichum gloeosporioides* is involved in copper transport and affects its germination and pathogenicity [15].

The present study characterizes *MLT1* of *C. albicans* belonging to the ABCC family. We demonstrate that, apart from PC (phosphatidylcholine) transport into the vacuolar lumen, the *MLT1* levels affect endocytosis, sequestration of ROS (reactive oxygen species), hypha formation and virulence implying its unconventional roles.

MATERIALS AND METHODS

Materials

The growth media YEPD (yeast extract/peptone/dextrose), serum and LB broth (LB) were purchased from Himedia. YNB (yeast nitrogen base) medium was purchased from Difco. $CuSO_4$, $NiSO_4$, KCl, KNO_3, $FeCl_3$, $CaCl_2$, $MgCl_2$ and H_2O_2 were obtained from Qualigens. The drug MTX (methotrexate) and chemicals Ficoll-400, BSA, sodium azide, phosphocreatine, creatine kinase, quinacrine, DCFDA (2′,7′-dichlorofluorescein diacetate), sucrose, Tris buffer, DMSO and MES were purchased from Sigma. FM4-64 (*N*-(3-triethylammoniumpropyl)-4-{6-[4-(diethylamino)phenyl] hexatrienyl} pyridinium ibromide) and NBD-PC (1-myristoyl-2-{6-[(7-nitro-2-1,3-benzoxadiazol-4-yl)amino]hexanoyl}-*sn*-glycero-3-phosphocholine) were obtained from Life Technologies and Avanti Polar Lipids respectively. HRP (horseradish peroxidase)-conjugated anti-His monoclonal antibody was purchased from Santa Cruz Biotechnology. BCA protein estimation kit was obtained from G Biosciences. The oligonucleotides used in the present study, as listed in Table 1, were obtained from Sigma Genosys.

Growth media and strains

All of the yeast strains were grown and maintained in YEPD and YNB media according to the experiment requirements. Spot assays were performed in YEPD agar medium with or without indicated treatment. Glycerol stock of strains were made in 15 % glycerol and maintained at − 80 °C and freshly revived in YEPD before use. Table 2 lists all of the strains used. All plasmids were maintained in the bacterial strain *Escherichia coli* DH5α as a host for the construction and propagation. *E. coli* cells were grown in LB medium containing 0.1 mg/ml ampicillin (Amresco).

Table 1   List of primers used in the present study

FP, forward primer; RP, reverse primer.

Primer name	Primer sequence
YBT1 null FP	5′-GCAGCTAATATAAACAAGTGATC-3′
YBT1 null RP	5′-CGACTGGAATATTGAAGTTAACGG-3′
YBT1 del con FP	5′-CTAAAGAAAAAGCCACTCAAG-3′
YBT1 del con RP	5′-CTTCGCGCCGTGCGGCCATC-3′
MLT1-PacI FP	5′-CGCGATTAATTAAATGAATGAACTGAATAGAGAACTTATC-3′
MLT1-NotI RP	5′-CGCGAGCGGCCGCAATCTATGTATCCACCTTCTTTGGC-3′
MLT1-K710A FP	5′-AAAGTTGGAAGTGGGGCATCTACTTTGATTAAG-3′
MLT1-K710A RP	5′-CTTAATCAAAGTAGATGCCCCACTTCCAACTTT-3′
Hgt12 FP	5′-GTTGTTATGGCTGTCTCCCAA-3′
Hgt12 RP	5′-CCACAAATAGCCCAACAAAGA-3′
SIT1 FP	5′-AATCCATTGGGGTTGAAAAAG-3′
SIT1 RP	5′-ACATCCGACAATCTGGCATAG-3′
NAD4 FP	5′-TGTATCTCCGCAGGTATAATGG-3′
NAD4 RP	5′-GCTAATAGCATTGAACCAGCAA-3′
FGR46 FP	5′-TGAACAAGGGCAGAAAGAAGA-3′
FGR46 RP	5′-GCAATCAGACGCAGTTGAAAT-3′
AOX2 FP	5′-CCTTCGTCATTTGCATTCATT-3′
AOX2 RP	5′-AATTTCCCAGGAACAGCAAGT-3′
ROY1 FP	5′-CAACTACTACCGTCGTTGGGA-3′
ROY1 RP	5′-ACTCGTCCAAATCTCCAAGGT-3′
RTA4 FP	5′-TTCTATAGCGGCTCAACGGTA-3′
RTA4 RP	5′-TGGTCGACCTCGTAAATCTTG-3′
RTA2 FP	5′-CAGTTTTGAAGCCAATGTGGT-3′
RTA2 RP	5′-TTATCGAACGTCGACCATAGG-3′
CSH1 FP	5′-GTCAAAGACGACGCAGAAGAC-3′
CSH1 RP	5′-TTTGCAACTCAACAAATTCCC-3′
OYE32 FP	5′-CCAATTGTCGATTACGCTCAT-3′
OYE32 RP	5′-TTCTAGCAGCAGCACCAAAAT-3′
ACT1 FP	5′-GGGTAGGGTGGGAAAACTTCA-3′
ACT1 RP	5′-TTGAAACCACTGCCGACAGA-3′

MLT1 plasmid construction

The *MLT1* gene was amplified using MLT1-PacI FP and MLT1-NotI RP primers (Table 1) from the genomic DNA of strain SC5314. The PCR product was inserted into PacI/NotI-digested pABC3GFP and pABC3His vectors [16]. Positive clones were confirmed by sequencing. Mutant variants of the WT (wild-type) *MLT1* gene were made by site-directed mutagenesis using a QuikChange® Site-Directed Mutagenesis Kit from Agilent Technology following the manufacturer's instructions [2]. Mutations were introduced into plasmids pABC3-Mlt1-GFP and pABC3-Mlt1-His using the primers MLT1-K710A FP and MLT1-K710A RP (Table 1). The mutations were confirmed by sequencing. The mutated plasmids were maintained in *E. coli* DH5α cells.

Strain construction

AD-RP strain construction

A *YBT1* gene deletion cassette along with the KanamaX selection marker gene was amplified from a *YBT1*-null strain using primers YBT1 null FP and YBT1 null RP (Table 1). To construct an AD-RP strain, *S. cerevisiae* AD1-8u⁻ strain was transformed with the PCR product using the lithium acetate method, and transformants were selected on YEPD plates with 25 μg/ml geneticin (Amresco). Genomic DNA was isolated from the putative colonies, and gene deletion was confirmed by using *YBT1*-null confirmation primers (Table 1).

Table 2   List of strains used in the present study

Strain	Genotype/description	Source/reference
WT(SC5314)	Wild-type strain	[59]
mlt1Δ/MLT1 (ST13-9)	ST13 derivative, Δmlt1-1::hisG/MLT1	[43]
mlt1Δ/Δ (ST13-63)	ST13-12 derivative, Δmlt1-1::hisG/Δmlt1-2::hisG	[43]
mlt1Δ/Δ::MLT1 (ST13-K2)	ST13-63 derivative, Δmlt1-1::hisG/MLT1-MPA^R	[43]
C4GFP	CAI4 derivative, MLT1/MLT1::GFP-URA3	[43]
AD-RP	AD1-8U⁻ derivative (Mata,pdr1-3,ura3 his1, Δyor1::hisG, Δsnq2::hisG, Δpdr5::hisG, Δpdr10::hisG, Δpdr11::hisG, Δycf1::hisG, Δpdr3::hisG, Δpdr15::hisG, Δybt1:: kanMX)	The present study
AD-RP-Mlt1p-GFP	AD-RP cells harbouring MLT1 ORF fused with GFP integrated at the PDR5 locus	The present study
AD-RP-K710A Mlt1p-GFP	AD-RP-Mlt1p-GFP cells harbouring K710A mutation in MLT1 ORF and integrated at the PDR5 locus	The present study
AD-RP-Mlt1p-HIS	AD-RP cells harbouring MLT1 ORF fused with a His tag integrated at the PDR5 locus	The present study
AD-RP-K710A Mlt1p-HIS	AD-RP-Mlt1p-HIS cells harbouring K710A mutation in MLT1 ORF and integrated at the PDR5 locus	The present study

MLT1 overexpression strains

To construct strains overexpressing WT (pABC3-Mlt1-GFP and pABC3-Mlt1-His) and mutant variants (pABC3-Mlt1-K710A-GFP and pABC3-Mlt1-K710A-His), plasmids were digested with AscI. The resultant transformation cassettes were used to transform AD-RP cells using the lithium acetate method and selected for uracil prototrophy [16,17].

Bioinformatic analysis

The topology of Mlt1p was predicted using the online software TOPOCONS, and a cartoon was prepared [18,19]. Phylogenetic analysis was carried out using MEGA 6 software.

Spot dilution growth assays

The susceptibility of strains towards various drugs and chemicals was tested by serial dilution spot assays essentially as described previously [20]. In summary, the strains were grown overnight on YEPD agar plates, and cultures were diluted to a D_{600} of 0.1 in 0.9 % saline. From this culture, further 5-fold serial dilutions were made, and 5 μl of cells from each dilution was spotted on to a YEPD agar plate with test chemicals for growth inhibition, and the plates were incubated at 30 °C for 48 h. Each experiment was repeated two or three times. Representative images are shown.

NBD-PC-accumulation assay

The NBD-PC-transport study was carried out in early-exponential-phase cells, as described previously [21]. Early-exponential-phase cells in YNB medium were incubated with 10 μM NBD-PC for 30 min at 30 °C with shaking (200 rev./min). Then, the cells were centrifuged at 2319.85 g and washed twice with YNB medium at room temperature. For the visualization of vacuoles, cells were resuspended in 2 ml of YEPD medium to which 20 μM FM4-64 was added and incubated for 1 h at 30 °C with shaking. After incubation, the cells were washed twice with ice-cold YNB and sodium azide, and slides were prepared for fluorescence microscopy.

Mlt1p expression and ATPase activity assay

Purified vacuoles (100 μg) were separated by SDS/PAGE (8 % gel) and transferred to membrane. The membrane was immunodetected with HRP-conjugated anti-His monoclonal antibody (Santa Cruz Biotechnology) as described previously [2]. After immunodetection, the membrane was stained with Ponceau S solution and used as a loading control.

For ATPase activity measurement, purified vacuoles (10 μg) were used in an enzymatic assay as described previously [22]. In summary, this assay couples ATP hydrolysis to the oxidation of NADH. The oxidized NADH can be measured as the loss of absorbance at 340 nm. The reaction mixture was incubated at 30 °C for 1 h. The vacuole ATPase activity of the AD-RP strain was subtracted from both the WT and mutant version of Mlt1p-overexpressing strains to assess ATPase activity specific to Mlt1p.

In vitro NBD-PC-transport assay

Vacuoles were purified as described previously using a ficoll density gradient method from *C. albicans* WT (SC5314) and *mlt1*Δ/Δ mutant [23] and kept at 4 °C. The NBD-PC-uptake assay was performed on freshly prepared vacuolar vesicles at 30 °C, as described previously [21]. Uptake was studied in intact vacuoles, which were selected on the basis of limiting membrane staining with FM4-64.

Lipid analysis

Lipid extraction and analyses was performed using an ESI source on a triple quadrupole mass spectrometer (ESI–MS/MS) (API 4000, Applied Biosystems), using methods described previously [24]. All experiments were performed in triplicate and results are shown as means $\pm$ S.E.M.

Transcriptome analysis

C. albicans strains were grown overnight in YEPD in biological duplicates. From primary cultures, cells at a D_{600} of 0.2 were inoculated into 15 ml of YEPD and allowed to grow for 6 h to reach exponential phase. The cells were pelleted down at 8228.48 g and washed with DEPC (diethyl pyrocarbonate)-treated water. RNA was isolated using an RNeasy Mini Kit (Qiagen) following the manufacturer's instructions. The concentration and purity of RNA samples were estimated using a nanodrop spectrophotometer and bioanalyser. Genotypic Technology performed microarray and data scanning. The threshold value was set to 2-fold to filter out only significantly affected genes. The transcription profile was analysed using the Go-Slim mapper and was annotated on the basis of biological processes [25].
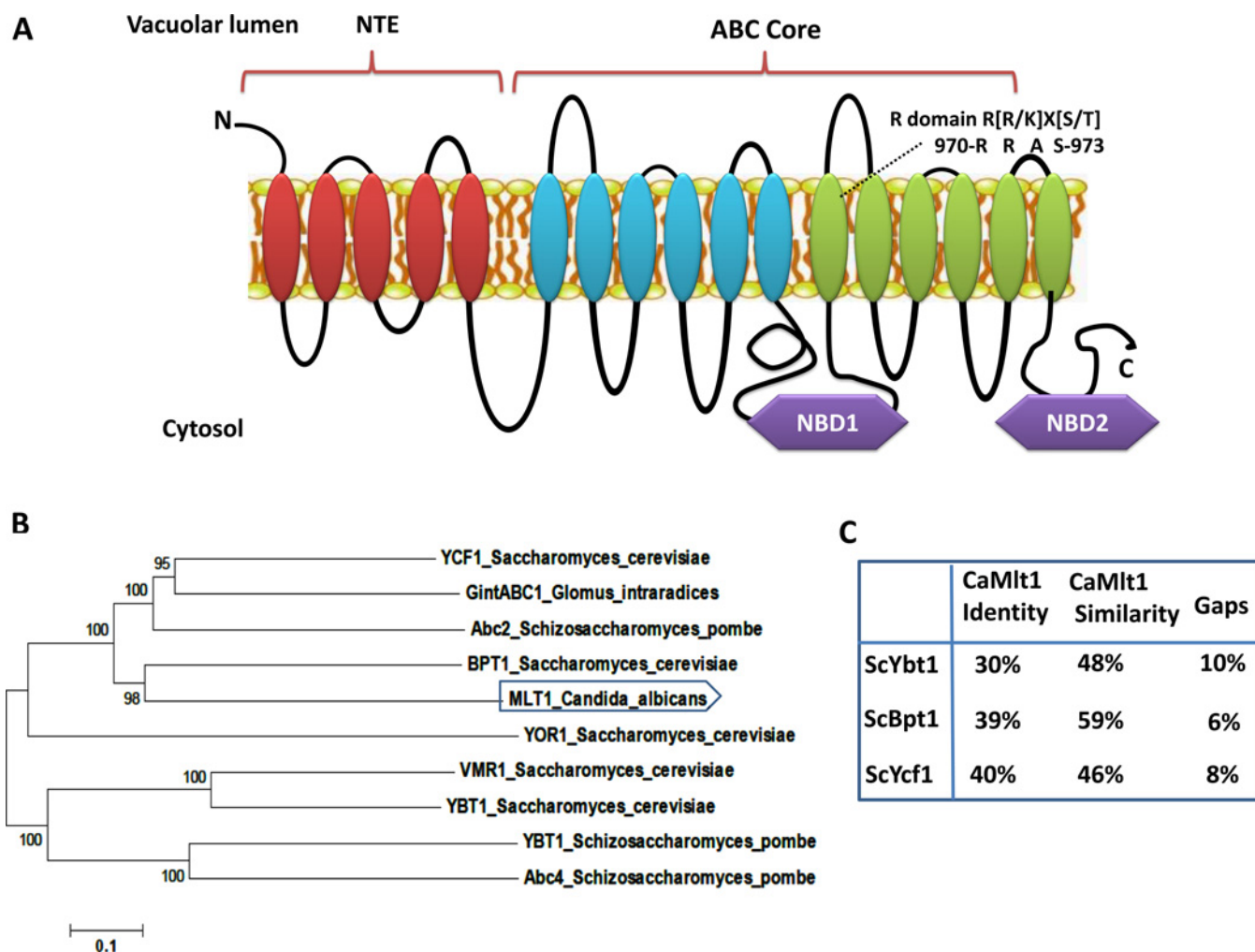
Figure 1   Bioinformatic analysis of the Mlt1p transporter of *C. albicans*

(**A**) Pictorial representation of the putative topology of Mlt1p as predicted by TOPCONS software showing typical domain arrangement of MRPs including a regulatory domain (R-domain) in TMH 12. NTE, N-terminal extension. (**B**) Phylogenetic analysis of *C. albicans* Mlt1p with yeast ABCC/MRP transporters of known functions. The analysis shows that the Mlt1p transporter is closest to the Bpt1 transporter of *S. cerevisiae*. The phylogenetic tree was generated using MEGA 6 software. Values at nodes represent bootstrap values signifying confidence levels. (**C**) BLASTp analysis of Mlt1p and *S. cerevisiae* vacuolar MRP transporters (ScYbt1, ScBpt1 and ScYcf1) of known functions.

Microarray accession number

The microarrays used in the present study along with complete transcriptome data can be accessed from the NCBI Gene Expression Omnibus database under accession number GSE70341.

FM4-64 endocytosis and live-cell imaging

C. albicans cells were stained with the lipophilic dye FM4-64. Cells were grown to exponential phase and incubated in 20 μM FM4-64 dye at static condition at room temperature. An aliquot of 50 μl was withdrawn at different time points to monitor the internalization of the stain.

To monitor time-lapse FM4-64 dye endocytosis in *C. albicans*, early-exponential-phase cells were mixed with 20 μM FM4-64 and fixed on microscopy slides with 2% agarose in YNB. The slide was kept inside a chamber that was maintained at 30°C for timelapse imaging under a Nikon Eclipse TiE microscope equipped with an Andor iXON3 EMCCD camera and controlled using Andor iQ2.7 software. Image acquisition was started 10 min

after the addition of dye and was monitored for a total duration of 3 h with a frequency of one image capture every 3 min.

Analysis of secretory protease activity

Extracellular protease activity was assayed on YBD (yeast/BSA/dextrose) plates [26]. Overnight cultures were washed with PBS and set to a D_{600} of 1 for each strain. A total of 5 μl of culture was spotted on a YBD plate (BSA agar plate) and incubated at 30°C for 5 days. After 5 days, a plate image was captured by a Bio-Rad ChemiDoc™ XRS + System, and the diameter of the halo zone surrounding the colony and colony diameter were measured using the quantification tool; halo diameters were normalized to the diameter of the fungal colony, where a value of 1 indicates no halo zone.

Measurement of ROS levels

The oxidant-sensitive probe DCFDA was used to measure endogenous ROS [27]. Cells were set to a D_{600} of 0.1 in
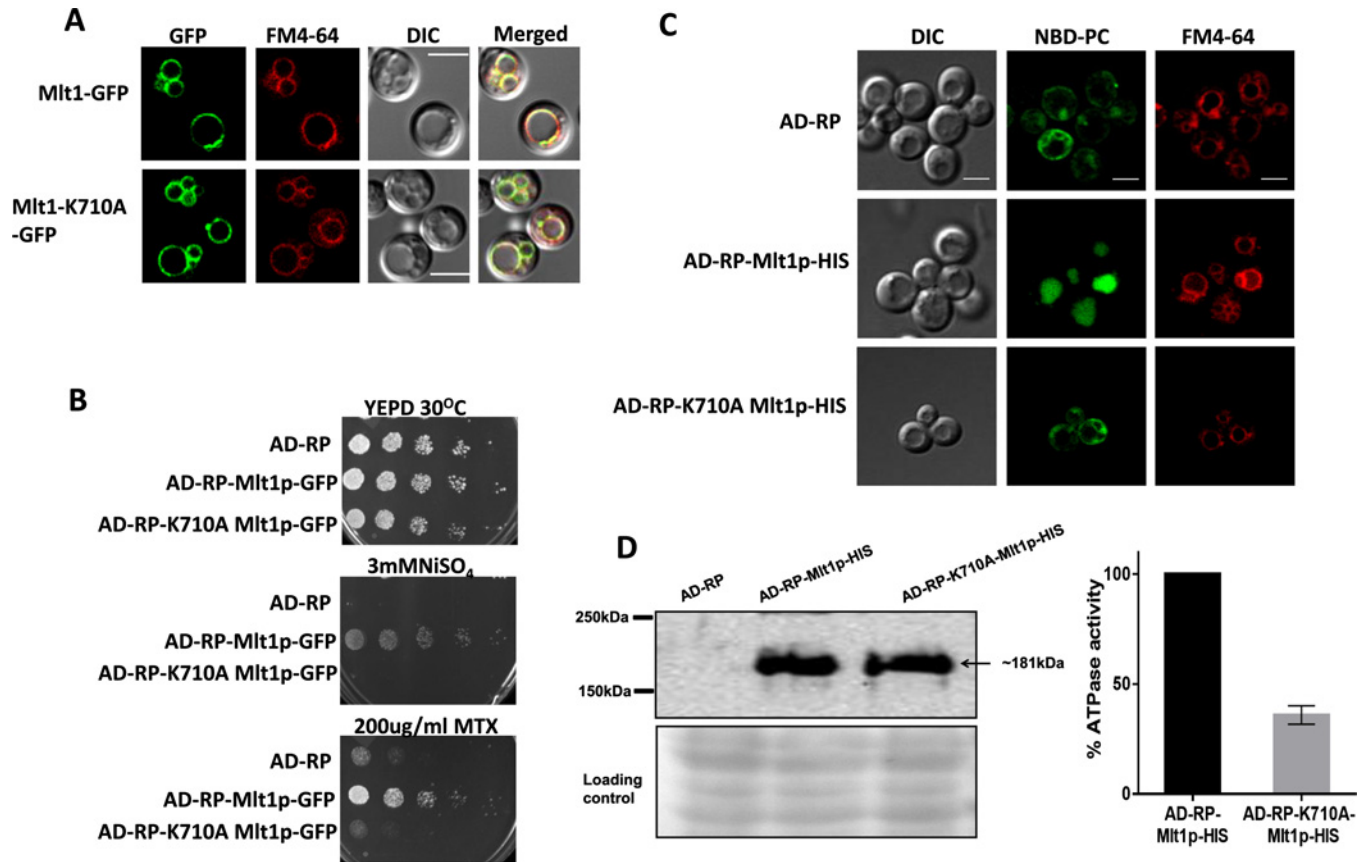
Figure 2 Expression, localization and characterization of WT Mlt1p and its mutant variant in a heterologous overexpressing strain

(**A**) Fluorescence imaging by confocal microscope (right-hand panel) showing VM localization of Mlt1p–GFP and Mlt1p-K710A–GFP proteins with corresponding differential interference contrast (DIC) images, FM4-64 staining and merged images. Scale bar, 10 μm. (**B**) A comparison by spot dilution assays of susceptibilities of overexpressing strains AD-RP-Mlt1p-GFP, AD-RP-K710A Mlt1p-GFP with parental AD-RP strain. A 5-fold serial dilution of each strain was spotted on to NiSO$_4$ and MTX at the indicated concentrations, in YEPD agar plates and grown for 48 h at 30°C. (**C**) NBD-PC accumulates in vacuolar lumen of WT Mlt1p-His-overexpressing strain (AD-RP-Mlt1p-HIS). Overexpression strains AD-RP-Mlt1p-HIS, AD-RP- K710A Mlt1p-HIS and parental strain AD-RP were grown to mid-exponential phase and incubated with NBD-PC. After incubation, cells were washed and stained with FM4-64. Samples were prepared for microscopy and photographed under a confocal microscope. Scale bar, 10 μm. (**D**) Immunoblot (left-hand panel) showing expression of Mlt1p-K710A–His and WT Mlt1p–His proteins. Vacuoles were isolated using the Ficoll gradient method and equal amounts of proteins (100 μg) were resolved by SDS/PAGE (8% gel) and then probed with anti-His antibody. After probing, membrane was stained with Ponceau S which is used as a loading control. ATPase activities (right-hand panel) in purified vacuolar vesicles from AD-RP-Mlt1p-HIS and AD-RP-Mlt1p-K710A-HIS strains were measured using an enzyme assay coupled to NADH oxidation at 340 nm. ATP hydrolysis is 60% reduced in Mlt1p-K710A-HIS mutants. Results are means $\pm$ S.D. ($n = 3$).

YEPD medium and incubated for 4 h at 30°C with shaking at 200 rev./min. Then, a 4 mM final concentration of H$_2$O$_2$ was added, and the culture was grown for 2 h. The cells were then divided into two equal parts. One half of the cells was analysed with a FACSCalibur flow cytometer (Becton Dickinson Immunocytometry Systems) at 495 nm excitation and 529 nm emission (filter FL1). A total of 10000 events were considered. The remaining cells were used to prepare slides and were observed under confocal microscopy with a FITC filter.

Whole blood killing assay

C. albicans strains SC5314, *mlt1*Δ/Δ and *mlt1*Δ/Δ::*MLT1* were grown overnight in YEPD at 30°C, re-inoculated into fresh YEPD and grown at 30°C to mid-exponential-phase. The cells were harvested in PBS and diluted to an appropriate concentration. Human whole blood was freshly drawn from healthy volunteers and anticoagulated with recombinant hirudin (Sarstedt), which does not influence complement activation. Immediately, yeast cells were added at a concentration of 10^6 cells/ml of whole blood

and incubated at 37°C for 4 h. After incubation, samples were instantly diluted in ice-cold water and plated on YEPD agar.

Morphogenic studies

Hyphae were induced on solid and liquid media as described previously [28]. Briefly, overnight cultures of *C. albicans* strains were washed with PBS and set to a D_{600} of 1. A total of 10 μl of cells was spotted on solid medium (spider, 10% serum), and the plates were incubated at 37°C for 3 or 6 days. Images were taken under a Nikon SMZ 1500 microscope. The experiment was repeated at least three times. Representative images are shown. For a liquid hyphal assay, exponential-phase cells at a D_{600} of 1 were diluted to a D_{600} of 0.5 with different hypha-inducing media and incubated in a 12-well plate at 37°C. Images were captured at the indicated time points.

Mouse survival assay

For all mouse experiments, female BALB/c mice (6 weeks old; Charles River) were housed in ventilated cages with free access
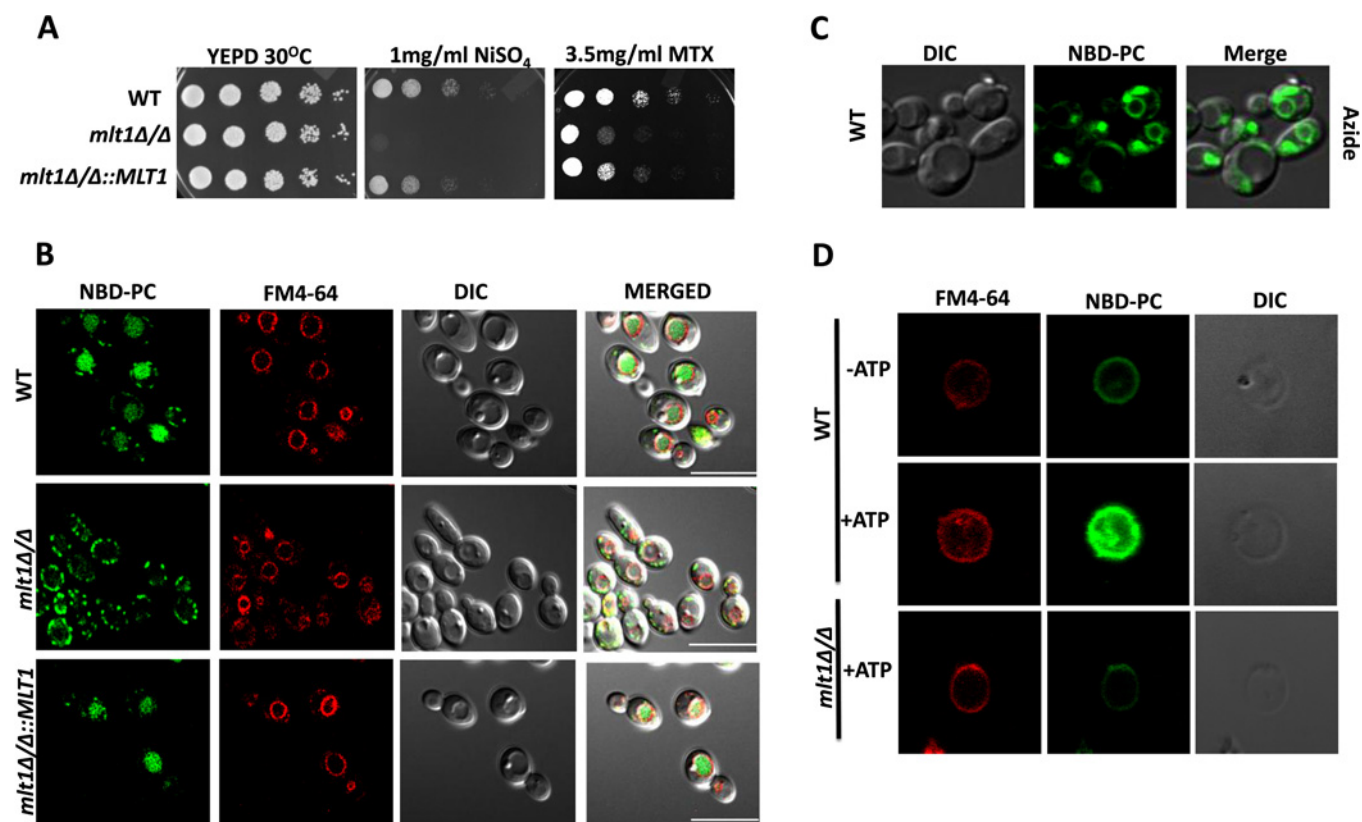
Figure 3   Mlt1p levels are required to maintain growth in the presence of NiSO$_4$, methotrexate and for accumulation of NBD-PC into the vacuolar lumen

(**A**) Comparison of growth by spot dilution assays of *C. albicans* WT (SC5314), *mlt1Δ/Δ* and *mlt1Δ/Δ::MLT1* cells. A 5-fold serial dilution of each strain was spotted on to NiSO$_4$ and MTX at the indicated concentrations, in YEPD agar plates and grown for 48 h at 30°C. (**B**) Deletion of *MLT1* results in the loss of accumulation of NBD-PC in the vacuolar lumen. *C. albicans* WT (SC5314), *mlt1Δ/Δ* and *mlt1Δ/Δ::MLT1* cells were grown to mid-exponential phase and incubated with NBD-PC. After incubation, cells were washed and stained with FM4-64. Samples were prepared for microscopy and photographed under a confocal microscope. Scale bar, 10 μm. (**C**) NBD-PC accumulation into the vacuolar lumen of *C. albicans* is energy-dependent. Sodium azide treatment was given to mid-exponential-phase WT *C. albicans* (SC5314) cells before their incubation with NBD-PC. The cells were photographed under a confocal microscope. (**D**) NBD-PC accumulation into the vacuolar lumen is energy-dependent. Vacuoles were isolated from WT and *mlt1Δ/Δ* mutant *C. albicans* using a Ficoll gradient ultracentrifuge-based method. Equal amounts (25 μg) of purified vacuolar vesicles were then incubated at 30°C for 30 min in buffer containing 10 μM NBD-PC and 10 μM FM4-64. A transport assay was carried out under two conditions: one in the absence of energy source ATP and another in the presence of 5 mM ATP. After incubation, samples were washed with ice-cold Tris/sucrose buffer containing 3 % fatty-acid-free BSA and observed under a confocal microscope. In the presence of ATP, the isolated vacuoles from WT *C. albicans* showed NBD-PC accumulation. There was no NBD-PC accumulation in the absence of ATP in WT cells and in vacuoles isolated from *mlt1Δ/Δ* mutant. DIC, differential interference contrast.

to food and water. Yeast strains were grown in individual tubes for 16 h under agitation at 30°C in YEPD medium. Each strain was subsequently diluted 100-fold in YEPD medium and grown overnight under agitation at 30°C. Overnight cultures were washed twice with PBS and resuspended in 5 ml of PBS. The concentration of each culture was measured by determination of the attenuance (D_{600}), and each strain was diluted in PBS to the desired concentration.

For survival experiments with single strain infections, groups of seven to ten mice were used. The mice were injected through the lateral tail vein with 250 μl of a cell suspension containing 2×10^6 cells/ml. The weight and health of the animals were monitored daily. The post-infection day of natural death or killing of moribund animals was recorded for each mouse. Survival experiments were terminated at 15 days after infection.

Statistical analysis

Differences in secreted protease activity were compared by one-way ANOVA followed by Tukey's post-hoc test. $P < 0.001$ is represented by ***. A two-tailed unpaired Student's t test was used for comparison of expression of Mlt1p between H$_2$O$_2$-treated and untreated cells, where $P = 0.007$ is represented by ***. Statistically significant lipid changes were highlighted by the pattern recognition tools such as PCA (principal component analysis) using the software XLSTAT (Addinsoft). A statistical significance value of 0.05 was employed using Student's t test in lipid species changes.

Ethics statement

All survival assay animal experiments were performed at the University Hospital Center of Lausanne with approval through the Institutional Animal Use Committee, Affaires Vétérinaires du Canton de Vaud, Switzerland (authorization numbers 1734.2 and 1734.3), according to decree 18 of the federal law on animal protection. For all mice experiments, female BALB/c mice (6 weeks old) were housed in ventilated cages with free access to food and water.

Human peripheral blood was collected from healthy volunteers who gave written informed consent. This study was conducted according to the principles expressed in the Declaration of Helsinki. The blood donation protocol and use of blood for this
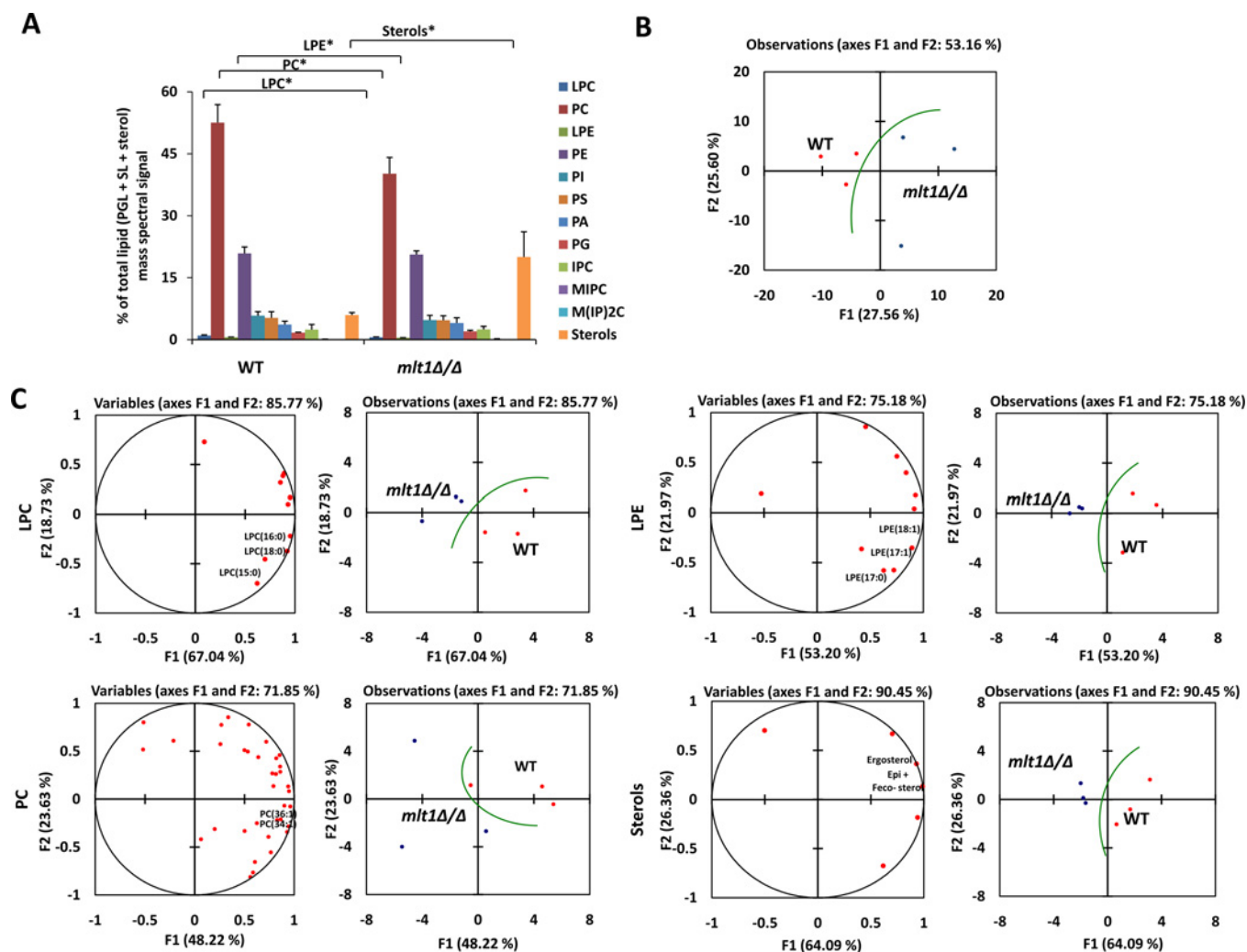
Figure 4   Deletion of Mlt1p results in altered lipid homoeostasis

(**A**) Lipid profile of *mlt1Δ/Δ* mutant compared with WT. The values represent the percentage of total PGL (phosphoglycerides) + SL (sphingolipids) + sterol mass spectral signal. Results are means ± S.E.M. (*n* = 3). *$P < 0.05$ (Student's *t* test). (**B**) PCA analysis of all lipid species analysed shows that the three replicates are grouped into WT (red) and *mlt1Δ/Δ* mutant (blue); and that their lipid profiles are different. Factors F1 (*x*-axis) and F2 (*y*-axis) represent the two most variable principal components. (**C**) PCA analyses of LPC, LPE, PC and sterols. PCA loading plots (left) represent the contribution of individual species to the sample variability. PCA plots showing the grouping of replicates are on the right. LPC, lysophosphatidylcholine; PC, phosphatidylcholine; LPE, lysophosphatidylethanolamine; PE, phosphatidylethanolamine; PI, phosphatidylinositol; PS, phosphatidylserine; PA, phosphatidic acid; PG, phosphatidylglycerol; IPC, inositol phosphorylceramide; MIPC, mannosylinositol phosphorylceramide; M(IP)₂C, mannosyldi-inositol phosphorylceramide.

study were approved by the institutional ethics committee of the University Hospital Jena (permission number 2207-01/08).

RESULTS

The topology prediction of Mlt1p suggests that its domain arrangement is similar to that of other MRPs (MDR proteins). It has a characteristic extra TMD (transmembrane domain) composed of five TMHs (transmembrane helices). Thus, similar to other proteins of the MRP subfamily, Mlt1p has a TMH₅-(TMD-NBD)₂ arrangement as depicted in Figure 1(A). Phylogenetic analysis of Mlt1p with functionally characterized fungal MRP (ABCC) subfamily members revealed its close resemblance to ScBpt1, a vacuolar transporter in *S. cerevisiae* (Figure 1B). Furthermore, BLASTp analysis with functionally characterized *S. cerevisiae* vacuolar transporters highlights that Mlt1p shows close sequence homology with *S. cerevisiae* ScBpt1p (39 % identity,

59 % similarity), ScYcf1p (40 % identity, 46 % similarity) and ScYbt1p (30 % identity, 48 % similarity) (Figure 1C).

Overexpression of Mlt1p in *S. cerevisiae*

For functional characterization, we used the *S. cerevisiae* AD1-8u⁻ strain as a heterologous expression system, which lacks seven major ABC transporters, including ScYor1p, ScSnq2p, ScPdr5p, ScPdr10p, ScPdr11p, ScYcf1p and ScPdr15p, thus resulting in hypersusceptibility to drugs [29]. This host expression system AD1-8u⁻ was derivatized further by the deletion of *ScYBT1* (an ion and drug transporter). The resulting strain was designated AD-RP. Because the well-characterized vacuolar transporters ScYcf1p and ScYbt1p are involved in drug transport, the deletion of *YBT1* from the AD1-8u⁻ background provided an overexpression system (AD-RP) with a cleaner background, ensuring minimum masking effects due to major ABC transporters of the host. Thus AD-RP, which is the derivative of AD1-8u⁻, not only lacks six
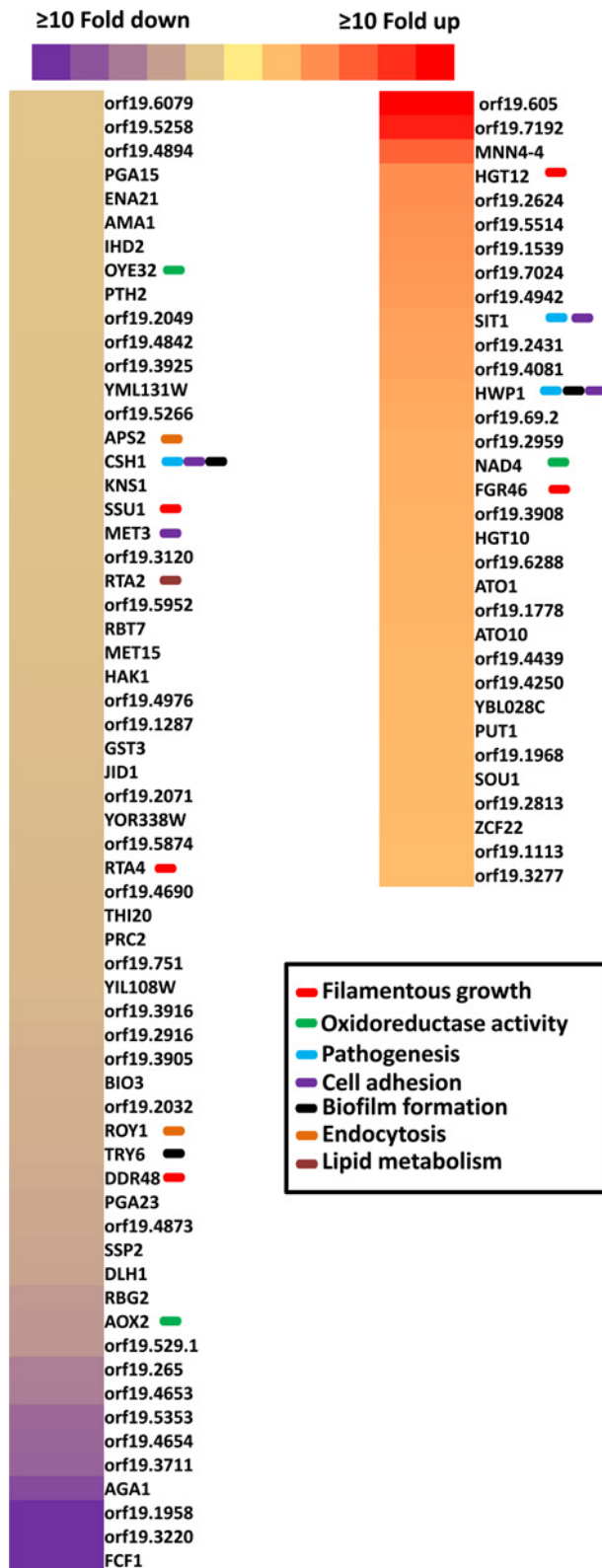
Figure 5   The comparative transcriptomic profile of *mlt1Δ/Δ* mutant

The genes with ≥2-fold change are shown. The intensity of the colour represents the extent of change in the expression values with red for up-regulation and violet for down-regulation as per the scale. The affected genes involved in endocytosis, oxidoreductase, lipid metabolism, hyphal development, biofilm formation, pathogenesis and adherence are labelled with a colour box. The different colour box represents different gene categories.

PM (plasma membrane)-localized ABC transporters (ScSnq2p, ScPdr5p, ScPdr10p, ScPdr11p, ScYor1p and ScPdr15p), but also is also devoid of two major vacuolar transporters (ScYcf1p and ScYbt1). *MLT1* was cloned into the vectors pABC3-GFP and pABC3-His and integrated into strain AD-RP to give strains AD-RP-Mlt1p-GFP and AD-RP-Mlt1p-HIS expressing Mlt1p from the *PDR5* locus. This strain exhibits a *pdr1-3* allele with a gain-of-function mutation in the transcription factor PDR1, resulting in constitutive high expression of Mlt1p [30]. The localization of overexpressed recombinant Mlt1p in AD-RP-Mlt1p-GFP was confirmed by confocal microscopy by employing the VM (vacuolar membrane)-specific fluorescent dye FM4-64 and was visualized using a TRITC filter (red fluorescence). The green fluorescence of GFP-tagged Mlt1p distinctly showed a rimmed appearance, specifically on the VM, which merged with the red fluorescence of FM4-64. The merged image clearly showed yellow fluorescence, which confirmed the localization of Mlt1p–GFP in the VM (Figure 2A, upper panel).

Mlt1p levels affect susceptibility to NiSO₄ and MTX

We performed growth assays with the Mlt1p–GFP protein overexpression strain on solid agar medium containing different ions such as $CuSO_4$, $NiSO_4$, KCl, KNO_3, $FeCl_3$, $CaCl_2$ and $MgCl_2$. There was no growth difference between the Mlt1p–GFP protein-overexpressing strain (AD-RP-Mlt1p-GFP) and the parental strain (AD-RP) in the majority of the conditions tested (results not shown). However, the overexpression of Mlt1p–GFP resulted in resistance to $NiSO_4$ compared with the parental AD-RP strain. Figure 2(B) depicts that the Mlt1p–GFP protein overexpressing strain AD-RP-Mlt1p-GFP could grow on up to 3 mM $NiSO_4$ compared with the parental strain AD-RP, which showed no growth at this concentration. Notably, the growth of the strain overexpressing Mlt1p–GFP protein (AD-RP-Mlt1p-GFP) remained unaffected in the presence of various other compounds (results not shown). However, it did show increased resistance towards MTX compared with the parental AD-RP strain (Figure 2B).

Mlt1p transports NBD-PC into the vacuolar lumen

We examined whether Mlt1p of *C. albicans* could transport phospholipids into vacuoles. For this, we exploited fluorescent NBD-PC to monitor PC accumulation inside vacuoles. Because fluorescence overlaps between the NBD tag of PC and the GFP tag of Mlt1p, we performed the NBD-PC-accumulation assays by using the Mlt1p–His-tagged overexpression strain (AD-RP-Mlt1p-HIS) and comparing it with the parental AD-RP strain (Figure 2C). It was evident that the fluorescent NBD-PC specifically accumulated within the vacuolar lumen of AD-RP-Mlt1p-HIS cells, which was confirmed further by the vacuole-specific dye FM4-64, whereas the parental strain AD-RP showed no NBD-PC fluorescence in the vacuolar lumen (Figure 2C).

Deletion of *MLT1* affects NiSO₄ and MTX susceptibility

As mentioned above, the *S. cerevisiae MLT1*-overexpressing strain showed resistance to $NiSO_4$ and MTX. We therefore addressed whether the deletion of *MLT1* in *C. albicans* would show the reverse phenotype. Serial dilution assays of *C. albicans* WT *mlt1Δ/Δ* and *mlt1Δ/Δ::MLT1* isolates on $NiSO_4$ and MTX revealed that *MLT1* was contributing to $NiSO_4$ and MTX resistance. The susceptibility towards both
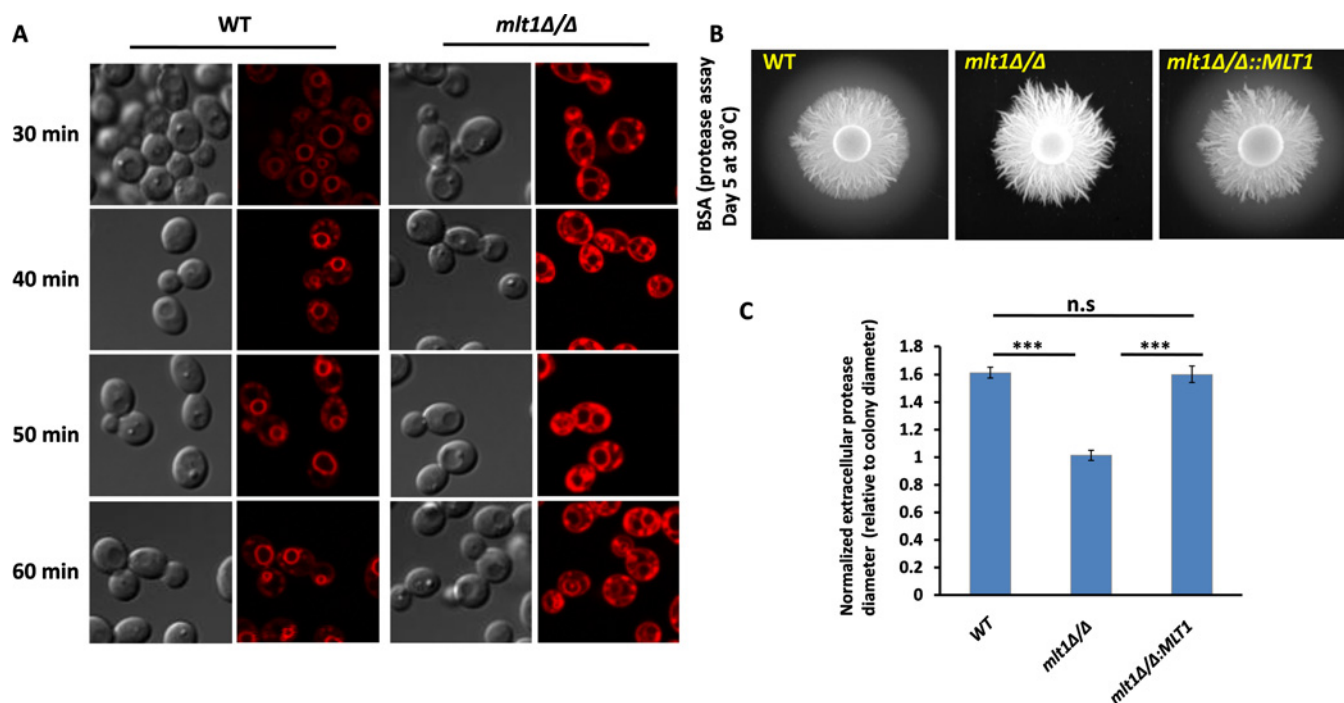
Figure 6   *mlt1Δ/Δ* mutant shows a delay in endocytosis of the lipophilic dye FM4-64 and loss of secreted protease activity

(**A**) Endocytosis process was studied using FM4-64 dye in WT and *mlt1Δ/Δ* mutant of *C. albicans*. Exponential-phase cells were incubated in 20 μM FM4-64 for 30, 40, 50 or 60 min under static conditions and monitored for internalization of the stain. In the case of WT, most of the dye was internalized by the endocytosis process and can be seen at the VM, whereas in the *mlt1Δ/Δ* mutant, the dye remained restricted either at the PM or between the VM and PM. (**B**) Overnight cultures were spotted on to BSA agar plates and grown at 30°C for 5 days. The zone of BSA degradation surrounding the fungal colony represents the secreted protease activity. Representative images are shown for WT, *mlt1Δ/Δ* and *mlt1Δ/Δ::MLT1* strains. (**C**) The quantification of secreted protease activity was made by measuring the diameter of the degradation halo surrounding the fungal colony and was normalized to the diameter of the colony itself, thus a ratio of 1 indicates a lack of detectable halo. Results are means $\pm$ S.E.M. Halo size is shown as the average for $n = 7$ replicates. ***$P < 0.001$ for WT compared with *mlt1Δ/Δ* and *mlt1Δ/Δ* compared with *mlt1Δ/Δ::MLT1* strains calculated by one-way ANOVA followed by Tukey's post-hoc test.

compounds in *mlt1Δ/Δ* was partially reversed in revertant isolates *mlt1Δ/Δ::MLT1* (Figure 3A).

MLT1 from *C. albicans* is involved in the transport of NBD-PC

Examination of the NBD-PC-accumulation capacity of vacuoles in *C. albicans* strains revealed that WT *C. albicans* was able to accumulate NBD-PC into the vacuolar lumen (Figure 3B, top panel); however, the *mlt1Δ/Δ* strain did not show any accumulation of NBD-PC, as was evident from the absence of NBD-PC fluorescence within the vacuolar lumen. Indeed, complementation of the null strain with a single allele of *MLT1* could restore NBD-PC accumulation within the vacuolar lumen (Figure 3B).

NBD-PC transport by Mlt1p into vacuoles is energy-dependent

Mlt1p is an ABC transporter, and it is expected that it drives ATP hydrolysis. We checked the energy-dependence of NBD-PC accumulation using two independent approaches. In the first instance, we performed the NBD-PC-accumulation assay in WT *C. albicans* (SC5134) cells treated with sodium azide. As depicted in Figure 3(C), it is clear that, following sodium azide treatment, which inhibited ATP hydrolysis, the WT *C. albicans* cells lost their ability to accumulate NBD-PC into the vacuolar lumen. We also used the AD-RP-Mlt1p-HIS and AD-RP-Mlt1p-GFP strains and changed a well-conserved and critical lysine residue of the Walker A motif of NBD1 (G^{704}KVGSG**K**S^{711}) to alanine by site-directed mutagenesis. This conserved lysine residue has been reported to

be important for ATP catalysis in many studies [21,31,32], and replacement of it with alanine (K710A) severely reduced ATPase activity (Figure 2D, right-hand panel) and abolished NBD-PC accumulation into vacuoles (Figure 2C). As expected, the mutant variant (K710A)-overexpressing strain also displayed enhanced susceptibility to NiSO$_4$ and MTX (Figure 2B). Confocal images of a strain expressing AD-RP-K710A Mlt1p-GFP confirmed that the K710A mutation did not affect Mlt1p localization. This eliminated the possibility that the inability to accumulate NBD-PC and susceptibility to NiSO$_4$ and MTX in the Mlt1p mutant variant could be due to mislocalization of the mutant variant protein (Figure 2A, lower panel). We performed Western blotting with vacuoles isolated from the AD-RP-Mlt1p-HIS and AD-RP-K710A Mlt1p-HIS strains to show that K710A Mlt1p–His was expressed and localized properly (Figure 2D, left-hand panel).

Mlt1p could transport NBD-PC into the vacuolar lumen *in vitro*

To strengthen the above results that Mlt1p transports NBD-PC and that this process is energy-dependent, we performed an *in vitro* NBD-PC-transport assay in a cell-free system using isolated vacuoles. For this, we grew *C. albicans* and the *mlt1Δ/Δ* mutant to exponential phase in YEPD medium and isolated vacuoles by density gradient centrifugation [23]. FM4-64 staining was performed to assess the integrity of the vacuoles. It is evident from Figure 3(D) that the isolated vacuoles were intact and could accumulate NBD-PC in the presence of 5 mM ATP, whereas this was not the case with vacuoles isolated from the *mlt1Δ/Δ* strain (Figure 3D, bottom panel).
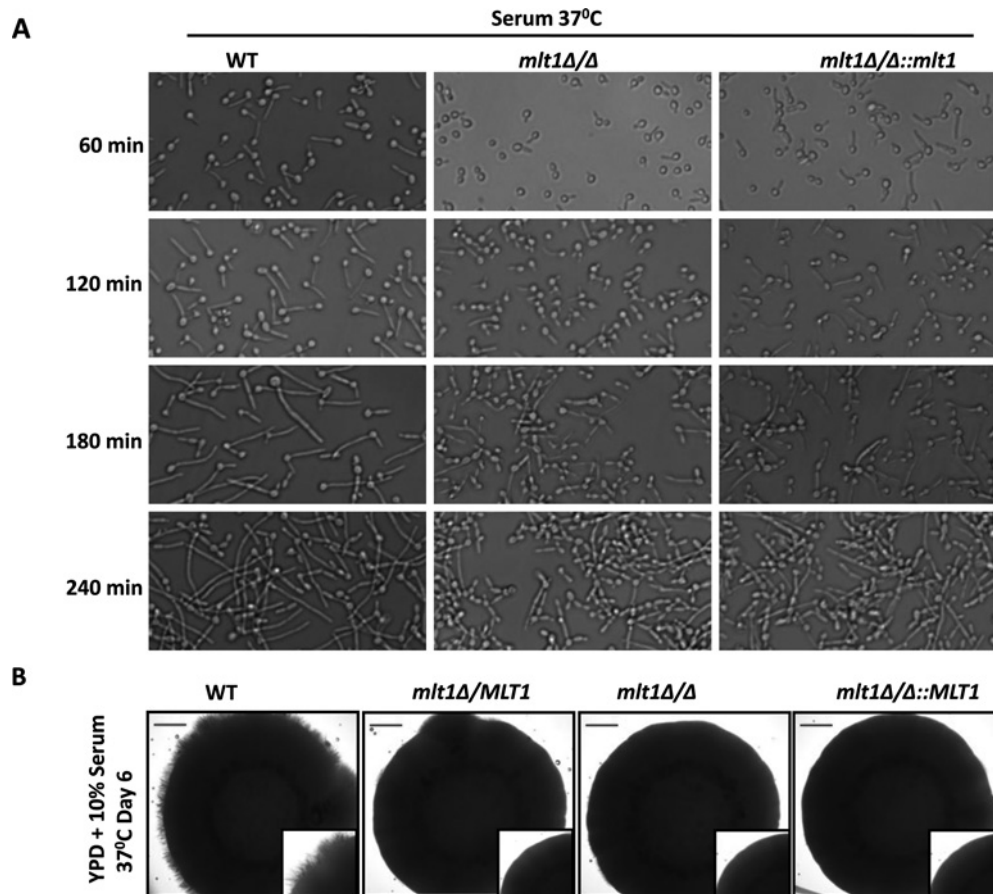
Figure 7   Deletion of *MLT1* affects hyphal growth in *C. albicans*

(**A**) *C. albicans* WT (SC5314), *mlt1Δ/Δ* and *mlt1Δ/Δ::MLT1* were incubated in liquid YEPD medium containing 10 % serum at 37 °C and images were captured after 60, 120, 180 or 240 min of incubation. (**B**) *MLT1* mutant becomes haploinsufficient on solid hypha-inducing medium. *C. albicans* WT (SC5314), *MLT1/mlt1Δ*, *mlt1Δ/Δ* and *mlt1Δ/Δ::MLT1* strains were spotted on to YEPD containing 10 % serum agar plates and incubated at 37 °C for 6 days. Scale bar, 100 μm.

Disruption of *MLT1* leads to altered lipid homoeostasis

Lipid homoeostasis by ABC transporters is very important in different organisms. For example, a large number of human genetic disorders related to ABC transporters are due to defects in lipid transport [33]. In the yeast *S. cerevisiae*, MRP family transporters such as ScYbt1 and ScYor1 are involved in PC and PE (phosphatidylethanolamine) translocation respectively [21,29]. ScYbt1 is able to accumulate PC into the lumen of the vacuole and is involved in phospholipid metabolism in *S. cerevisiae* cells [21]. Mlt1p, which translocates PC into the vacuolar lumen, could also affect lipid homoeostasis. We explored this possibility by performing high-throughput MS-based lipidome analysis of WT and *mlt1Δ/Δ* strains using ESI–MS/MS.

Our analysis showed that the lipid profile of the *mlt1Δ/Δ* mutant was indeed different from that of WT (Figures 4A and 4B). The *mlt1Δ/Δ* mutant showed depletion of PC, LPC (lysophosphatidylcholine) and LPE (lysophosphatidylethanolamine) content compared with WT (Figure 4A). These data suggest that deletion of *MLT1* alters the overall phospholipid homoeostasis of the cell. A closer look at the lipid species in the *mlt1Δ/Δ* mutant and WT using the PCA tool suggested significant modulation of molecular lipid species. The most notable differences were observed among mono-unsaturated ($LPE_{18:1}$, $LPE_{17:1}$, $PC_{34:1}$ and $PC_{36:1}$) and saturated ($LPC_{16:0}$, $LPC_{15:0}$, $LPE_{17:0}$, $LPC_{18:0}$) lipid species (Figure 4C).

The *mlt1Δ/Δ* strain transcriptome revealed differential expression of genes related to lipid homoeostasis, endocytosis, oxidative stress, hyphal development, biofilm formation and virulence

Because ABC transporters perform various physiological roles, we conducted a genome-wide transcriptome analysis of *mlt1Δ/Δ* in comparison with the WT. The transcription profile was analysed using CGD Go-slim mapper and was annotated on the basis of biological processes (Supplementary Figures S1A and S1B). The comparative transcriptomic profile revealed that the *mlt1Δ/Δ* strain showed up- and down-regulation ($\geqslant$2-fold) of 33 and 63 genes respectively (Figure 5). Notably, the differentially regulated transcripts in the *mlt1Δ/Δ* mutant included genes involved in endocytosis (*ROY1* and *APS2*), oxidoreductase (*OYE32*, *AOX2* and *NAD4*), lipid metabolism (*RTA2*), hyphal development (*SSU1*, *RTA4*, *DAD48*, *HGT12* and *FGR46*), biofilm formation, pathogenesis and adherence (*CSH1*, *TRY6*, *SIT1* and *HWP1*) as shown in Figure 5. The expression of some randomly selected genes was validated by semi-quantitative reverse transcription (RT)–PCR (Supplementary Figure S1C).

The *mlt1Δ/Δ* mutant shows a delay in endocytosis

Transcriptome data analysis revealed that gene products involved in endocytosis were down-regulated in the *mlt1Δ/Δ* mutant.
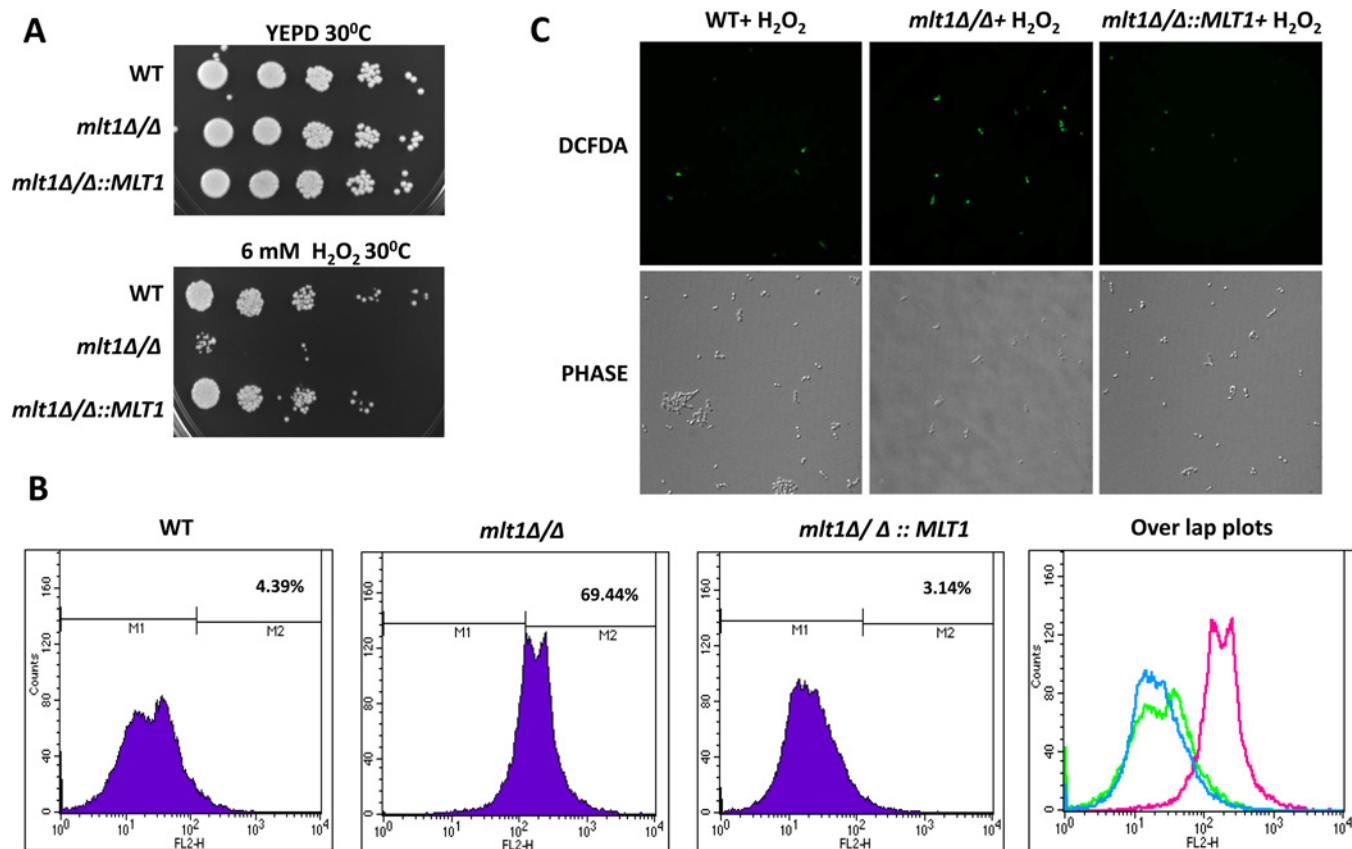
Figure 8   *MLT1* mutant is susceptible to oxidative stress by H_2O_2 and shows low ROS sequestration

(**A**) Comparison of growth by spot dilution assays of *C. albicans* WT (SC5314), *mlt1Δ/Δ* and *mlt1Δ/Δ::MLT1* cells. A 5-fold serial dilution of each strain was spotted on to 6 mM H_2O_2-containing YEPD agar and YEPD control and grown for 48 h at 30°C. (**B**) Measurement of ROS generation by FACS analysis using DCFDA in WT (SC5314), *mlt1Δ/Δ* and *mlt1Δ/Δ::MLT1* cells after treatment with sub-lethal concentration 4 mM H_2O_2 for 2 h. $n = 10000$ cells for each sample. (**C**) Confocal images of aliquots of samples used in FACS to measure ROS by DCFDA in WT (SC5314), *mlt1Δ/Δ* and *mlt1Δ/Δ::MLT1*.

We investigated endocytosis in the WT and the *mlt1Δ/Δ* mutant using FM4-64, a lipophilic dye commonly used to visualize endocytosis by confocal microscopy [34]. The FM4-64 dye stained the VM distinctly in WT after 30 min of exposure (Figure 6A). However, in the *mlt1Δ/Δ* mutant, even after 60 min, most of the dye remained restricted either to the PM or between the VM and PM. The delay in FM4-64 endocytosis was confirmed by timelapse microscopy of WT and *mlt1Δ/Δ* mutant strains. WT cells began to show FM4-64 staining of the VM from 9 min onwards, which became distinctly visible within 30 min. In contrast with WT, the *mlt1Δ/Δ* cells began to show FM4-64 staining of VM only after 90 min of incubation (Supplementary Figure S2).

The *mlt1Δ/Δ* mutant displays reduced secretory protease activity

A previous study revealed that vacuolar proteins such as Vph1 could affect the release of secretory proteases in *C. albicans* [22]. We explored whether the Mlt1p vacuolar transporter levels could affect protease secretion. For this, an *in vitro* BSA plate assay for secretory protease activity was performed, wherein the amount of extracellular secreted enzyme activity was quantified by the size of haloes surrounding fungal colonies corresponding to a zone of BSA degradation [26]. As depicted in Figure 6(B), in comparison

with WT, no halo of protein degradation appeared in the *mlt1Δ/Δ* mutant, indicating a deficiency in secretory protease activity or secretion (Figure 6C). Notably, the defect in secretory protease activity/secretion was not associated with any change in vacuolar lumen pH as measured by quinacrine pH dye (results not shown).

Deletion of *MLT1* affects filamentous growth in *C. albicans*

Our microarray data showed a differential expression of hyphal development-related genes (*SSU1*, *RTA4*, *DAD48*, *HGT12* and *FGR46*) and prompted us to evaluate the hyphal development ability of the *mlt1Δ/Δ* mutant in various hypha-inducing conditions. In liquid hypha-inducing medium (serum, spider and RPMI 1640), we performed a time-course study of hypha formation. Up to 60 min, it was observed that only a few cells from the *mlt1Δ/Δ* mutant showed hypha formation. Only at later time points (120, 180 and 240 min) could hyphae be observed, although their lengths were shorter than those of both WT and *mlt1Δ/Δ::MLT1* cells. Thus deletion of *MLT1* delayed hypha formation (Figure 7A, and Supplementary Figures S3B and S3C). Notably, in solid YEPD and 10% serum medium, *MLT1* becomes haploinsufficient, as the single allele null strain *mlt1Δ/MLT1* also showed absence of hypha formation (Figure 7B). In spider solid medium, the single allele mutant (*mlt1Δ/MLT1*) showed hyphae
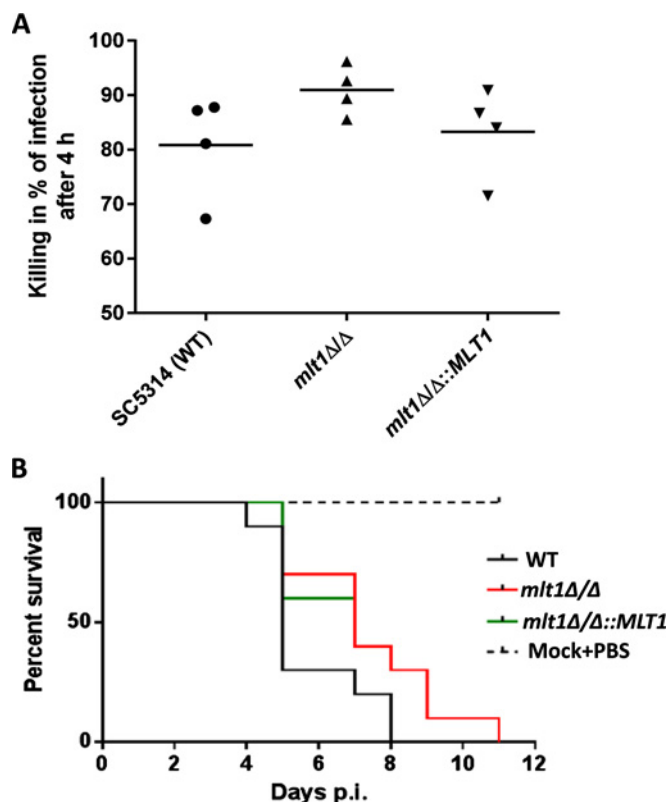
Figure 9   mlt1Δ/Δ mutant shows attenuation in virulence

(**A**) Killing assay for *C. albicans* WT (SC5314), *mlt1Δ/Δ* and *mlt1Δ/Δ::MLT1* cells in human whole blood after 4 h showing higher tendency of killing by the *mlt1Δ/Δ* mutant. (**B**) Survival curve of mice infected with *mlt1Δ/Δ* mutant shows attenuation in virulence as the mice infected with mutant strains survived up to 11 days post-infection compared with the WT *C. albicans* strains where all of the mice succumbed to infection within 8 days. Virulence was partially restored when a single copy of the *MLT1* gene was added back to mutants. p.i., post-infection.

but of shorter length (Supplementary Figure S3A). However, in embedded agar conditions, deletion of *MLT1* did not affect hypha formation (results not shown).

Yeast to hyphal switching can be considered an important virulence factor as mutants that are defective in filament formation show attenuated virulence [35]. The formation of hyphae and their active penetration are involved in host epithelial cell damage [36]. Because the *mlt1Δ/Δ* mutant was defective in hyphal formation, we compared the oral epithelial cell-damaging ability of WT, *mlt1Δ/Δ* and *mlt1Δ/Δ::MLT1* cells. However, we did not observe any significant difference in epithelial cell damage between these different cell types (results not shown).

The transcriptome profile and the hyphal formation data indicated that the *mlt1Δ/Δ* mutant could be defective in biofilm formation compared with WT. Different genes involved in biofilm formation, such as *CSH1*, *TRY6* and *HWP1*, are differentially expressed in the *mlt1Δ/Δ* mutant compared with WT. However, a close comparison of the biofilm-formation capacity of WT, *mlt1Δ/Δ* and *mlt1Δ/Δ::MLT1* strains in a rat catheter model did not show significant differences (results not shown). This may suggest that the observed down-regulation of gene expression in *mlt1Δ/Δ* could be a transient effect not directly associated with *MLT1*. Alternatively, since biofilm formation involves a complex regulatory network, the presence of overlapping genes could mask any detectable phenotype due to altered expression of few genes in *mlt1Δ/Δ* cells.

MLT1 deletion results in hypersusceptibility to oxidative stress and higher killing by human whole blood

We observed that some oxidoreductase activity-related genes (*OYE32*, *AOX2* and *NAD4*) are differentially regulated in the *mlt1Δ/Δ* mutant. We checked the survival of the *mlt1Δ/Δ* mutant in the presence of 6 mM H_2O_2 by serial dilution assays. Figure 8(A) depicts that, in contrast with WT and *mlt1Δ/Δ::MLT1*, the *mlt1Δ/Δ* strain was unable to grow at the H_2O_2 concentrations tested. This finding was well supported by ROS measurements where it was evident using DCFDA, an oxidant-sensitive probe, that the fluorescence of the dye was higher in *mlt1Δ/Δ* cells than in WT and *mlt1Δ/Δ::MLT1* cells (Figure 8B). The enhanced level of ROS in *mlt1Δ/Δ* cells was also reflected in fluorescence images that were examined simultaneously in another batch of cells withdrawn from the same suspension. It was apparent that *mlt1Δ/Δ* cells displayed enhanced fluorescence compared with WT and *mlt1Δ/Δ::MLT1* cells (Figure 8C), thus suggesting that the *MLT1*-null strain was not able to sequester ROS efficiently.

Once *C. albicans* enters the host bloodstream, neutrophils and macrophages play an important role in killing the fungus. ROS generation is one of the key mechanisms in the killing of pathogens by neutrophils. Although the percentage of killing in whole human blood did not show a large difference, there was a noticeable trend of higher killing after 4 h in the case of the *mlt1Δ/Δ* mutant (91.1 %) compared with WT (81.1 %) and *mlt1Δ/Δ::MLT1* (83.1 %) strains (Figure 9A). This may also explain the lower ROS-sequestering efficiency of *MLT1*-null strains (Figures 8B and 8C). However, we did not observe any difference in the killing of WT and *mlt1Δ/Δ* mutant by human primary macrophages (results not shown).

To determine the infection capacity of the *mlt1Δ/Δ* mutant, a mouse survival assay was performed. Immunocompetent BALB/c mice were infected with WT (SC5314), *mlt1Δ/Δ* and *mlt1Δ/Δ::MLT1* cells. A marked difference in the survival rate of mice infected with WT and *mlt1Δ/Δ* strains was observed. Some 70 % of mice infected with WT *C. albicans* died on day 5, peaking to 100 % death at day 8. In contrast with WT, among mice infected with the *mlt1Δ/Δ* mutant, only 30 % death was recorded at day 5, reaching 100 % only after day 11 (Figure 9B). Notably, mice infected with the revertant *mlt1Δ/Δ::MLT1* showed survival closer to the *mlt1Δ/Δ* mutant. This could be because the presence of both of the *MLT1* alleles is required for maintenance of the virulence trait as both alleles must be retained in order to maintain proper hypha formation (Figure 7).

H_2O_2 exposure enhances the level of Mlt1p–GFP

Because Mlt1p helps in the survival of *C. albicans* under H_2O_2 stress, we explored whether oxidative stress could also influence the expression of Mlt1p. For this, the fluorescence of GFP in GFP-tagged Mlt1p, which was expressed from its chromosomal locus in *C. albicans*, was quantified by two methods: by measuring ROI (region of interest) intensity using confocal microscopy and by a quantitative estimation of fluorescence using a spectrofluorimeter. The ROI mean intensity of the VM was calculated for approximately 40 cells from different fields. Figures 10(A) and 10(B) depict a statistically significant ($P = 0.007$) increase in ROI mean intensity in H_2O_2-treated cells. The Mlt1p–GFP fluorescence quantified using a spectrofluorimeter further supported the confocal microscopy data, revealing an increase of ∼2-fold in the fluorescence intensity following H_2O_2 treatment of *C. albicans* (Figure 10C).
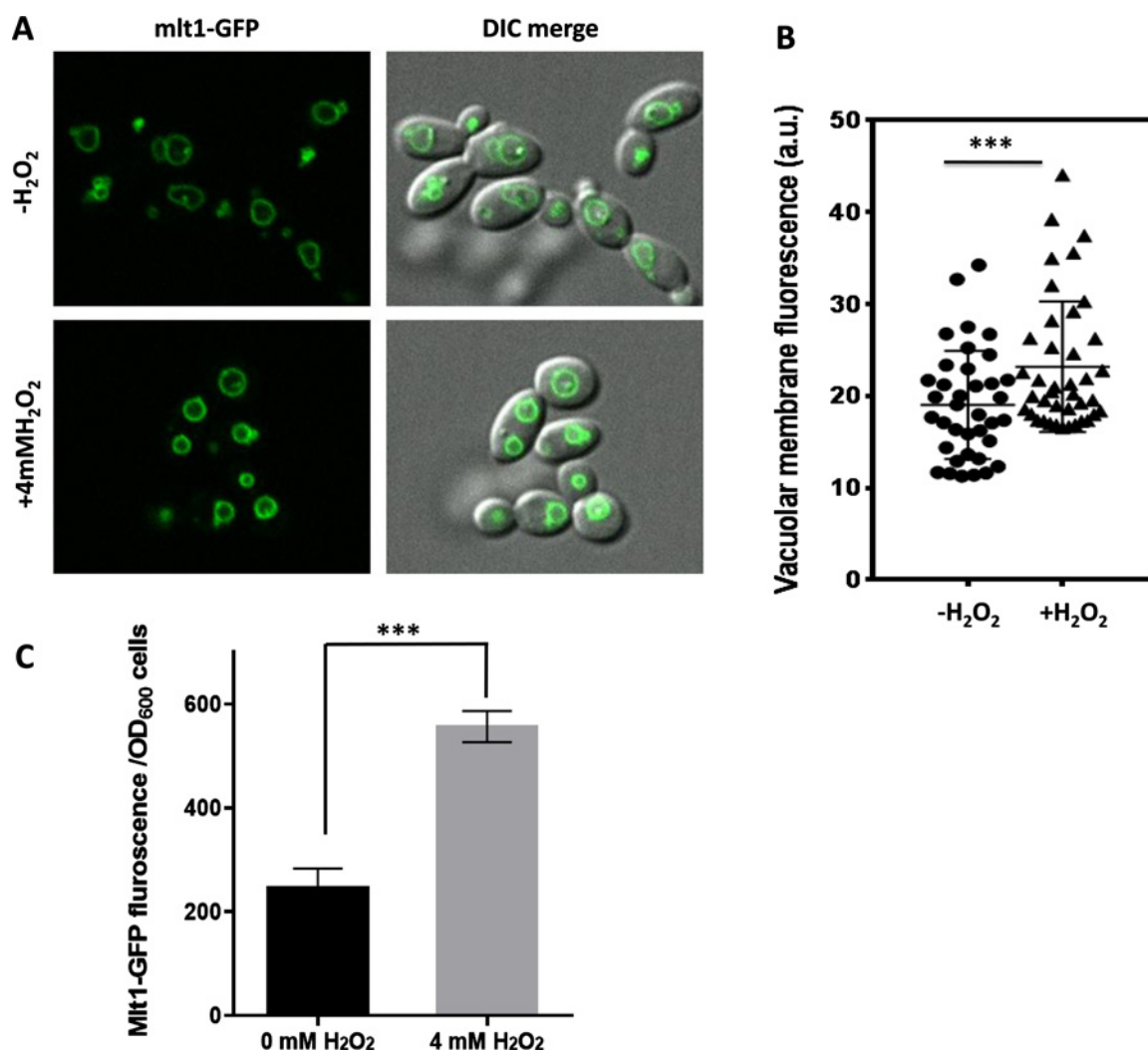
Figure 10   H$_2$O$_2$ treatment induces the expression of Mlt1p–GFP

(**A**) Exponential-phase cells of *C. albicans* expressing GFP-tagged Mlt1p from its chromosomal locus were grown further for 2 h with or without 4 mM H$_2$O$_2$. The cells were then washed with PBS and observed under a fluorescence microscope. Representative images are shown. (**B**) ROI intensity measured using NIS elements AR are plotted. Results are means $\pm$ S.E.M. ($n = 37$ for untreated and $n = 40$ for treated samples). Two-tailed unpaired Student's t test was used. ***$P = 0.007$. (**C**) Equal numbers of cells (D_{600} of 1) were set in PBS buffer in aliquots of samples treated for 2 h with or without 4 mM H$_2$O$_2$ and quantification of Mlt1p–GFP fluorescence was measured using a spectrofluorimeter. Results are means $\pm$ S.D. ***$P < 0.0004$ for mutant compared with WT strains as measured by unpaired Student's t test.

DISCUSSION

The members belonging to the MRP subfamily of ABC transporters from different organisms have different physiological roles such as transport of PC and PE lipids, ions, bile salt, glutathione (GS)-conjugated compounds, leukotriene C$_4$, glycocholic acid, cyclic nucleotides and *ade2* pigments; and in vacuole fusion and oxidative stress. [21,29,37–40]. Except for the PM-localized ScYor1, all of the remaining MRP members (ScYbt1, ScYcf1, ScBpt1, ScNft1 and ScVmr1) in *S. cerevisiae* are localized in the VM and transport different substrates, including ions, bile salt, GS-conjugated compounds and phosphoglycerides [21,41,42]. The commensal pathogenic *C. albicans* has four MRP family members, *MLT1*/orf19.5100, orf19.6478, orf19.6382, and orf19.1783, but none has been assigned any functional role. However, Mlt1p is one of the members of the MRP subfamily in *C. albicans* that is localized in the VM [43]. Our functional analysis in the present study revealed

that contrary to an earlier report, which suggested the absence of a *ScYBT1* homologue in *C. albicans* [44], *MLT1* appears to be a functional homologue of this transporter. For instance, similarly to *ScYBT1*, *MLT1* deletion not only results in complete loss of NBD-PC accumulation in the vacuolar lumen, but it also promotes enhanced susceptibility to NiSO$_4$ and MTX.

We observed that *MLT1* levels are critical for withstanding oxidative stress in *C. albicans*. Thus not only are *mlt1*Δ/Δ cells susceptible to H$_2$O$_2$ treatment, but also they have elevated levels of ROS, implying lower efficiency of the null strain in its sequestration. Of note, the *ScYCF1* transporter is known to be involved in oxidative stress [39]; our data also indicate that *MLT1* has such a role, a notion that is well reinforced by transcriptome data showing differential regulation of oxidative-stress-related genes (*OYE32*, *AOX2* and *NAD4*) in *mlt1*Δ/Δ cells. This result would imply that *MLT1* not only is able to functionally complement *ScYBT1*, but also can also partially perform the function of *ScYCF1*. Hence the vacuolar transporter *MLT1*
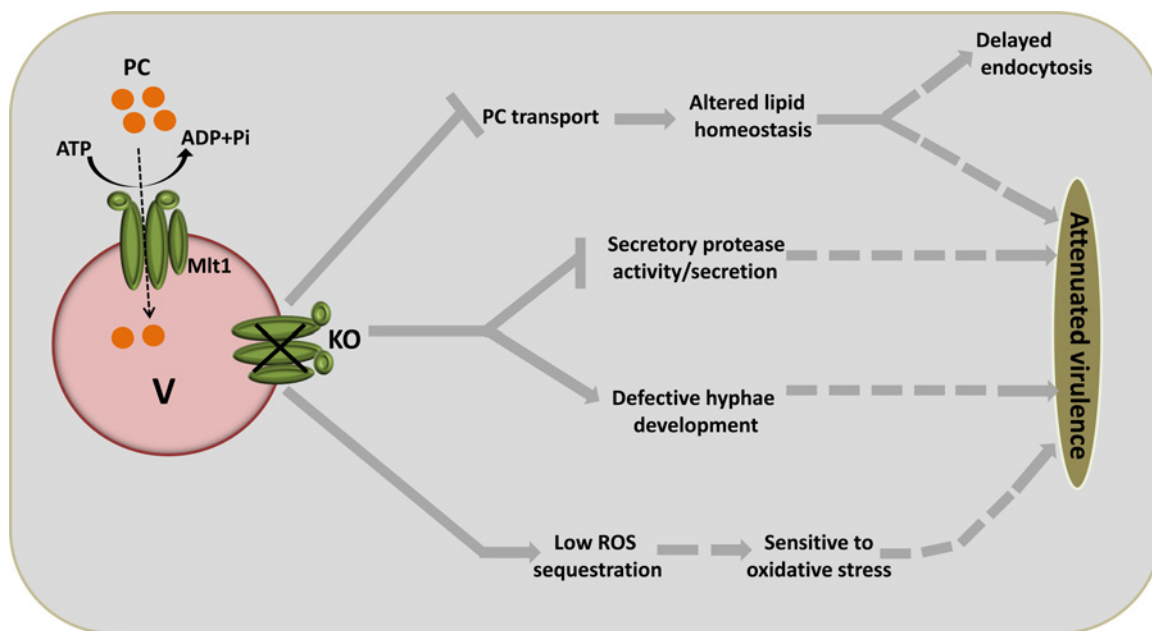
Figure 11   Proposed model for vacuolar Mlt1p transporter function and its roles in different phenotypes

Mlt1p which is localized to the VM transports the PC analogue NBD-PC into the vacuolar lumen in an energy-dependent manner and maintains lipid homoeostasis. Thus *MLT1* deletion may lead to defects in endocytosis and virulence. Deletion of *MLT1* also negatively affects various virulence related traits such as hyphae formation, secretory protease activity/secretion and sensitivity to oxidative stress. Thus all of these phenotypes show their cumulative effect to attenuated virulence in the *mlt1Δ/Δ* mutant.

is capable of performing dual functions, which are otherwise performed by two independent proteins in *S. cerevisiae*. This situation can probably justify the existence of fewer members of the MRP subfamily in the *C. albicans* genome compared with that of *S. cerevisiae*. Interestingly, the inventory of ABC proteins in the *C. albicans* genome did not identify any homologue of Sc*YBT1*; it did, however, indicate two putative ORFs, orf19.6478 and orf19.5100/*MLT1*, as Sc*YCF1* homologues. Although the former remains uncharacterized, we now report that part of the function of *S. cerevisiae* Sc*YCF1* is performed by *MLT1*. Together, the data from the present and previous studies rule out the existence of real homologues of Sc*YBT1* and Sc*YCF1* in *C. albicans*, which apparently is taken over by *MLT1* in parts.

Further functional analysis revealed that *MLT1* levels affect cellular endocytosis. For instance, as revealed by timelapse confocal microscopy, *mlt1Δ/Δ* cells displayed a significant delay in endocytosis (Figure 6A and Supplementary Figure S2). The involvement of an ABC transporter in endocytosis appears to be a novel function, but it is not surprising because, in different organisms, several members of the ABC family have diverse non-transport functions such as in metabolism, germination, pathogenicity, biofilm architecture, polarized growth, capsule synthesis and oxidative stress [8,11,12,15,39,45–48]. Notably, hyphal development in *C. albicans* is already known to be linked to endocytosis with proteins such as Vrp1, Vps1, Vph1, Pep12, Rvs161 and Rvs167 affecting endocytosis and hyphal development [22,49–53].

The behaviour of the *mlt1Δ/Δ* mutant with regard to hyphal development could also explain an earlier study wherein an Mlt1p–GFP fusion protein was used to study the effect of the Rab GTPase on Golgi-to-vacuole trafficking. It was reported that *vps21Δ/Δ* (vacuolar protein sorting Rab GTPase) cells of *C. albicans* showed defective hyphal formation on agar medium, and this phenotype was enhanced when another GTPase (*YPT52*)

was also deleted in the *vps21Δ/Δ* background. However, the deletion of *YPT52* alone in the WT did not affect hyphal formation [54]. Interestingly, in the double knockout (*vps21Δ/Δ*, *ypt52Δ/Δ*), a significant amount of Mlt1p was mislocalized. Considering our observations that deletion of even a single allele of *MLT1* (*mlt1Δ/MLT1*) can lead to a defect in hyphal development, it is thus plausible that the potentiation of hyphal defects by *YPT52* deletion in the *vps21Δ/Δ* null background could have been caused by Mlt1p mislocalization. Interestingly, the *mlt1Δ/Δ* mutant shows a delay in endocytosis and in parallel differential expression of hyphal development-related genes. Additionally, the *mlt1Δ/Δ* mutant showed attenuated virulence in an immunocompetent mouse model. Thus our results also support the well-established correlation between endocytosis, hyphal development and virulence.

Generally, phenotypes such as altered vesicle trafficking, oxidative stress and attenuated virulence are associated with defects in ergosterol biosynthesis in *C. albicans* [55–58]. Additionally, these phenotypes are also mimicked in vacuolar endocytosis mutants [22,49–51,53]. However, in the case of the *mlt1Δ/Δ* mutant, its high ergosterol content suggests that these phenotypes might be independent of the ergosterol pathway (Supplementary Table S1). High ergosterol content could rather be a compensatory change. Interestingly, this consideration emphasizes further that the role of Mlt1p is more attributable to PC transport into the vacuolar lumen.

In conclusion, Mlt1p transports PC into the vacuolar lumen, and it affects lipid homoeostasis, thus leading to delayed endocytosis, defects in hyphae and biofilm, susceptibility to drugs, protease activity/secretion, survival of oxidative stress and killing by whole blood, together culminating in attenuated virulence (Figure 11). The present study not only supports the well-known role of ABC transporters in MDR, but also provides strong evidence in support of multiple functional roles of a member of the ABC transporter superfamily in *C. albicans*.

AUTHOR CONTRIBUTION

ACKNOWLEDGEMENT

FUNDING

REFERENCES

1 White, T.C., Holleman, S., Dy, F., Laurence, F., Stevens, D.A. and Mirels, L.F. (2002) Resistance mechanisms in clinical isolates of *Candida albicans*. Antimicrob. Agents Chemother. **46**, 1704–1713 CrossRef

2 Shukla, S., Saini, P., Jha, S., Ambudkar, V., Prasad, R. and Ambudkar, S.V. (2003) Functional characterization of *Candida albicans* ABC transporter Cdr1p. Eukaryot. Cell **2**, 1361–1375 CrossRef PubMed

3 Liu, T.T., Znaidi, S., Barker, K.S., Xu, L., Homayouni, R., Saidane, S., Morschhäuser, J., Nantel, A., Raymond, M. and Rogers, P.D. (2007) Genome-wide expression and location analyses of the *Candida albicans* Tac1p regulon. Eukaryot. Cell **6**, 2122–2138 CrossRef PubMed

4 Sanglard, D., Ischer, F., Monod, M. and Bille, J. (1997) Cloning of *Candida albicans* genes conferring resistance to azole antifungal agents: characterization of *CDR2*, a new multidrug ABC transporter gene. Microbiology **143**, 405–416 CrossRef PubMed

5 Smriti, Krishnamurthy, S., Dixit, B.L., Gupta, C.M., Milewski, S. and Prasad, R. (2002) ABC transporters CdrLp, Cdr2p and Cdr3p of a human pathogen *Candida albicans* are general phospholipid translocators. Yeast **19**, 303–318 CrossRef PubMed

6 Young, L., Leonhard, K., Tatsuta, T., Trowsdale, J. and Langer, T. (2001) Role of the ABC transporter Mdl1 in peptide export from mitochondria. Science **291**, 2135–2138 CrossRef PubMed

7 Ketchum, C.J., Schmidt, W.K., Rajendrakumar, G.V., Michaelis, S. and Maloney, P.C. (2001) The yeast **a**-factor transporter Ste6p, a member of the ABC superfamily, couples ATP hydrolysis to pheromone export. J. Biol. Chem. **276**, 29007–29011 CrossRef PubMed

8 Wang, Y., Liu, T.B., Delmas, G., Park, S., Perlin, D. and Xue, C. (2011) Two major inositol transporters and their role in cryptococcal virulence. Eukaryot. Cell **10**, 618–628 CrossRef PubMed

9 Sanguinetti, M., Posteraro, B., La Sorda, M., Torelli, R., Fiori, B., Santangelo, R., Delogu, G. and Fadda, G. (2006) Role of *AFR1*, an ABC transporter-encoding gene, in the *in vivo* response to fluconazole and virulence of *Cryptococcus neoformans*. Infect. Immun. **74**, 1352–1359 CrossRef PubMed

10 Orsi, C.F., Colombari, B., Ardizzoni, A., Peppoloni, S., Neglia, R., Posteraro, B., Morace, G., Fadda, G. and Blasi, E. (2009) The ABC transporter-encoding gene *AFR1* affects the resistance of *Cryptococcus neoformans* to microglia-mediated antifungal activity by delaying phagosomal maturation. FEMS Yeast Res. **9**, 301–310 CrossRef PubMed

11 Cottrell, T.R., Griffith, C.L., Liu, H., Nenninger, A.A. and Doering, T.L. (2007) The pathogenic fungus *Cryptococcus neoformans* expresses two functional GDP-mannose transporters with distinct expression patterns and roles in capsule synthesis. Eukaryot. Cell **6**, 776–785 CrossRef PubMed

12 Paul, S., Diekema, D. and Moye-Rowley, W.S. (2013) Contributions of *Aspergillus fumigatus* ATP-binding cassette transporter proteins to drug resistance and virulence. Eukaryot. Cell **12**, 1619–1628 CrossRef PubMed

13 Yoshino, R., Morio, T., Yamada, Y., Kuwayama, H., Sameshima, M., Tanaka, Y., Sesaki, H. and Iijima, M. (2007) Regulation of ammonia homeostasis by the ammonium transporter AmtA in *Dictyostelium discoideum*. Eukaryot. Cell **6**, 2419–2428 CrossRef PubMed

14 Paul, J.A., Barati, M.T., Cooper, M. and Perlin, M.H. (2014) Physical and genetic interaction between ammonium transporters and the signaling protein Rho1 in the plant pathogen *Ustilago maydis*. Eukaryot. Cell **13**, 1328–1336 CrossRef PubMed

15 Barhoom, S., Kupiec, M., Zhao, X., Xu, J.R. and Sharon, A. (2008) Functional characterization of CgCTR2, a putative vacuole copper transporter that is involved in germination and pathogenicity in *Colletotrichum gloeosporioides*. Eukaryot. Cell **7**, 1098–1108 CrossRef PubMed

16 Lamping, E., Monk, B.C., Niimi, K., Holmes, A.R., Tsao, S., Tanabe, K., Niimi, M., Uehara, Y. and Cannon, R.D. (2007) Characterization of three classes of membrane proteins involved in fungal azole resistance by functional hyperexpression in *Saccharomyces cerevisiae*. Eukaryot. Cell **6**, 1150–1165 CrossRef PubMed

17 Gietz, R.D., Schiestls, R.H., Willems, A.R. and Woods, R.A. (1995) Studies on the transformation of intact yeast cells by the LiAc/SS-DNA/PEG procedure. Yeast **11**, 355–360 CrossRef PubMed

18 Bernsel, A., Viklund, H., Hennerdal, A. and Elofsson, A. (2009) TOPCONS: consensus prediction of membrane protein topology. Nucleic Acids Res. **37**, 465–468 CrossRef

19 Tsirigos, K.D., Peters, C., Shu, N., Kall, L. and Elofsson, A. (2015) The TOPCONS web server for consensus prediction of membrane protein topology and signal peptides. Nucleic Acids Res. **43**, W401–W407 CrossRef PubMed

20 Mukhopadhyay, K., Kohli, A. and Prasad, R. (2002) Drug susceptibilities of yeast cells are affected by membrane lipid composition. Antimicrob. Agents Chemother. **46**, 3695–3705 CrossRef PubMed

21 Gulshan, K. and Moye-Rowley, W.S. (2011) Vacuolar import of phosphatidylcholine requires the ATP-binding cassette transporter ybt1. Traffic **12**, 1257–1268 CrossRef PubMed

22 Raines, S.M., Rane, H.S., Bernardo, S.M., Binder, J.L., Lee, S.A. and Parra, K.J. (2013) Deletion of vacuolar proton-translocating ATPase Voa isoforms clarifies the role of vacuolar pH as a determinant of virulence-associated traits in *Candida albicans*. J. Biol. Chem. **288**, 6190–6201 CrossRef PubMed

23 Bankaitis, V.A., Johnson, L.M. and Emr, S.D. (1986) Isolation of yeast mutants defective in protein targeting to the vacuole. Proc. Natl. Acad. Sci. U.S.A. **83**, 9075–9079 CrossRef PubMed

24 Mahto, K.K., Singh, A., Khandelwal, N.K., Bhardwaj, N., Jha, J. and Prasad, R. (2014) An assessment of growth media enrichment on lipid metabolome and the concurrent phenotypic properties of *Candida albicans*. PLoS One **9**, e113664 CrossRef PubMed

25 Boyle, E.I., Weng, S., Gollub, J., Jin, H., Botstein, D., Cherry, J.M. and Sherlock, G. (2004) GO::TermFinder: open source software for accessing Gene Ontology information and finding significantly enriched Gene Ontology terms associated with a list of genes. Bioinformatics **20**, 3710–3715 CrossRef PubMed

26 Ross, I.K., De Bernardis, F., Emerson, G.W., Cassone, A. and Sullivan, P.A. (1990) The secreted aspartate proteinase of *Candida albicans*: physiology of secretion and virulence of aproteinase-deficient mutant. J. Gen. Microbiol. **136**, 687–694 CrossRef PubMed

27 Dhamgaye, S., Devaux, F., Vandeputte, P., Khandelwal, N.K., Sanglard, D., Mukhopadhyay, G. and Prasad, R. (2014) Molecular mechanisms of action of herbal antifungal alkaloid berberine, in *Candida albicans*. PLoS One **9**, e104554 CrossRef PubMed

28 Prasad, T., Saini, P., Gaur, N.A., Ram, A., Khan, L.A., Haq, Q.M.R. and Vishwakarma, R.A. (2005) Functional analysis of *CaIPT1*, a sphingolipid biosynthetic gene involved in multidrug resistance and morphogenesis of *Candida albicans*. Antimicrob. Agents Chemother. **49**, 3442–3452 CrossRef PubMed

29 Decottignies, A., Grant, A.M., Nichols, J.W., De Wet, H., McIntosh, D.B. and Goffeau, A. (1998) ATPase and multidrug transport activities of the overexpressed yeast ABC protein Yor1p. J. Biol. Chem. **273**, 12612–12622 CrossRef PubMed

30 Nakamura, K., Niimi, M., Niimi, K., Holmes, A.R., Yates, J.E., Decottignies, A., Monk, B.C., Goffeau, A. and Cannon, R.D. (2001) Functional expression of *Candida albicans* drug efflux pump Cdr1p in a *Saccharomyces cerevisiae* strain deficient in membrane transporters. Antimicrob. Agents Chemother. **45**, 3366–3374 CrossRef PubMed

31 Frelet, A. and Klein, M. (2006) Insight in eukaryotic ABC transporter function by mutation analysis. FEBS Lett. **580**, 1064–1084 CrossRef PubMed

32 Ren, X.-Q., Furukawa, T., Haraguchi, M., Sumizawa, T., Aoki, S., Kobayashi, M. and Akiyama, S. ((2004) Function of the ABC signature sequences in the human multidrug resistance protein 1. Mol. Pharmacol. **65**, 1536–1542 CrossRef PubMed

33 Paulusma, C.C. and Oude Elferink, R.P.J. (2006) Diseases of intramembranous lipid transport. FEBS Lett. **580**, 5500–5509 CrossRef PubMed

34 Vida, T.A. and Emr, S.D. (1995) A new vital stain for visualizing vacuolar membrane dynamics and endocytosis in yeast. J. Cell Biol. **128**, 779–792 CrossRef PubMed

35 Lo, H.J., Köhler, J.R., DiDomenico, B., Loebenberg, D., Cacciapuoti, A. and Fink, G.R. (1997) Nonfilamentous *C. albicans* mutants are avirulent. Cell **90**, 939–949 CrossRef PubMed

36 Wächtler, B., Wilson, D., Haedicke, K., Dalle, F. and Hube, B. (2011) From attachment to damage: defined genes of *Candida albicans* mediate adhesion, invasion and damage during interaction with oral epithelial cells. PLoS One **6**, e17046 CrossRef PubMed

37 Klein, M., Mamnun, Y.M., Eggmann, T., Schüller, C., Wolfger, H., Martinoia, E. and Kuchler, K. (2002) The ATP-binding cassette (ABC) transporter Bpt1p mediates vacuolar sequestration of glutathione conjugates in yeast. FEBS Lett. **520**, 63–67 CrossRef PubMed

38 Kruh, G.D. and Belinsky, M.G. (2003) The MRP family of drug efflux pumps. Oncogene **22**, 7537–7552 CrossRef PubMed

39 Lee, M.E., Singh, K., Snider, J., Shenoy, A., Paumi, C.M., Stagljar, I. and Park, H.O. (2011) The Rho1 GTPase acts together with a vacuolar glutathione S-conjugate transporter to protect yeast cells from oxidative stress. Genetics **188**, 859–870 CrossRef PubMed

40 Sasser, T.L., Lawrence, G., Karunakaran, S., Brown, C. and Fratti, R.A. (2013) The yeast ATP-binding cassette (ABC) transporter Ycf1p enhances the recruitment of the soluble SNARE Vam7p to vacuoles for efficient membrane fusion. J. Biol. Chem. **288**, 18300–18310 CrossRef PubMed

41 Li, Z.S., Szczypka, M., Lu, Y.P., Thiele, D.J. and Rea, P.A. (1996) The yeast cadmium factor protein (YCF1) is a vacuolar glutathione S-conjugate pump. J. Biol. Chem. **271**, 6509–6517 CrossRef PubMed

42 Sharma, K.G., Mason, D.L., Liu, G., Rea, P.A., Bachhawat, A.K. and Michaelis, S. (2002) Localization, regulation, and substrate transport properties of Bpt1p, a *Saccharomyces cerevisiae* MRP-type ABC transporter. Eukaryot. Cell **1**, 391–400 CrossRef PubMed

43 Theiss, S., Kretschmar, M., Nichterlein, T., Hof, H., Agabian, N., Hacker, J. and Köhler, G.A. (2002) Functional analysis of a vacuolar ABC transporter in wild-type *Candida albicans* reveals its involvement in virulence. Mol. Microbiol. **43**, 571–584 CrossRef PubMed

44 Kovalchuk, A. and Driessen, A.J.M. (2010) Phylogenetic analysis of fungal ABC transporters. BMC Genomics **11**, 177 CrossRef PubMed

45 Mayer, F.L., Wilson, D., Jacobsen, I.D., Miramón, P., Große, K. and Hube, B. (2012) The novel *Candida albicans* transporter Dur31 is a multi-stage pathogenicity factor. PLoS Pathog. **8**, CrossRef

46 Bishop, A.C. (2013), Transport and Metabolism of Glycerophosphodiesters by *Candida albicans*. Ph.D. Thesis, Duquesne University, Pittsburgh, PA, U.S.A

47 Shah, A.H., Singh, A., Dhamgaye, S., Chauhan, N., Vandeputte, P., Suneetha, K.J., Kaur, R., Mukherjee, P.K., Chandra, J., Ghannoum, M.A. et al. (2014) Novel role of a family of major facilitator transporters in biofilm development and virulence of *Candida albicans*. Biochem. J. **460**, 223–235 CrossRef PubMed

48 Tran, P.N., Brown, S.H.J., Mitchell, T.W., Matuschewski, K., McMillan, P.J., Kirk, K., Dixon, M.W.A. and Maier, A.G. (2014) A female gametocyte-specific ABC transporter plays a role in lipid metabolism in the malaria parasite. Nat. Commun. **5**, 4773 CrossRef PubMed

49 Barelle, C.J., Richard, M.L., Gaillardin, C., Gow, N.A.R. and Brown, A.J.P. (2006) *Candida albicans* VAC8 is required for vacuolar inheritance and normal hyphal branching. Eukaryot. Cell **5**, 359–367 CrossRef PubMed

50 Cornet, M., Bidard, F., Schwarz, P., Costa, D., Blanchin-roland, S. and Dromer, F. (2005) Deletions of endocytic components VPS28 and VPS32 affect growth at alkaline pH and virulence through both RIM101 pathways in *Candida albicans*. Infect. Immun. **73**, 7977–7987 CrossRef PubMed

51 Bernardo, S.M., Khalique, Z., Kot, J., Jones, J.K. and Lee, S.A. (2008) *Candida albicans* VPS1 contributes to protease secretion, filamentation, and biofilm formation. Fungal Genet. Biol. **45**, 861–877 CrossRef PubMed

52 Douglas, L.M., Martin, S.W. and Konopka, J.B. (2009) BAR domain proteins Rvs161 and Rvs167 contribute to *Candida albicans* endocytosis, morphogenesis, and virulence. Infect. Immun. **77**, 4150–4160 CrossRef PubMed

53 Palanisamy, S.K.A., Ramirez, M.A., Lorenz, M. and Lee, S.A. (2010) *Candida albicans* PEP12 is required for biofilm integrity and *in vivo* virulence. Eukaryot. Cell **9**, 266–277 CrossRef PubMed

54 Johnston, D.A., Tapia, A.L., Eberle, K.E. and Palmer, G.E. (2013) Three prevacuolar compartment Rab GTPases impact *Candida albicans* hyphal growth. Eukaryot. Cell **12**, 1039–1050 CrossRef PubMed

55 Mukherjee, P.K., Chandra, J., Kuhn, D.M. and Ghannoum, M.A. (2003) Mechanism of fluconazole resistance in *Candida albicans* biofilms: phase-specific role of efflux pumps and membrane sterols. Infect. Immun. **71**, 4333–4340 CrossRef PubMed

56 Thorpe, G.W., Fong, C.S., Alic, N., Higgins, V.J. and Dawes, I.W. (2004) Cells have distinct mechanisms to maintain protection against different reactive oxygen species: oxidative-stress-response genes. Proc. Natl. Acad. Sci. U.S.A. **101**, 6564–6569 CrossRef PubMed

57 Zhang, Y.Q., Gamarra, S., Garcia-Effron, G., Park, S., Perlin, D.S. and Rao, R. (2010) Requirement for ergosterol in V-ATPase function underlies antifungal activity of azole drugs. PLoS Pathog. **6**, e1000939 CrossRef PubMed

58 Landolfo, S., Zara, G., Zara, S., Budroni, M., Ciani, M. and Mannazzu, I. (2010) Oleic acid and ergosterol supplementation mitigates oxidative stress in wine strains of *Saccharomyces cerevisiae*. Int. J. Food Microbiol. **141**, 229–235 CrossRef PubMed

59 Mullaney, E.J., Hamer, J.E., Roberti, K.A., Yelton, M.M. and Timberlake, W.E. (1985) Primary structure of the *trpC* gene from *Aspergillus nidulans*. Mol. Gen. Genet. **199**, 37–45 CrossRef PubMed